# Representative point-integrated suspended sediment sampling in rivers

**by**

**Alessandro B. Gitto**

B.Sc., University of Western Ontario, 2012

Thesis Submitted in Partial Fulfillment of the
Requirements for the Degree of
Master of Science

in the
Department of Geography
Faculty of Environment



**SIMON FRASER UNIVERSITY**

**Fall 2015**

# Approval

| | |
|---|---|
| **Name:** | **Alessandro B. Gitto** |
| **Degree:** | **Master of Science (Geography)** |
| **Title:** | ***Representative point-integrated suspended sediment sampling in rivers*** |
| **Examining Committee:** | **Chair:** Nadine Schuurman<br>Professor |

**Jeremy Venditti**
Senior Supervisor
Associate Professor

**Michael Church**
Supervisor
Professor Emeritus
Department of Geography
University of British Columbia

**Ray Kostaschuk**
Supervisor
Adjunct Professor

**Brian Menounos**
External Examiner
Professor
Department of Geography
University of Northern British Columbia

**Date Defended/Approved:** September 29, 2015

## Abstract

Point-integrated bottle sampling is the traditional method to determine the mean concentration of suspended sediment. Sample duration is assumed to average over enough variability to represent the mean suspended sediment concentration. Inadequate time averaging in relation to point-integrated sampling remains unexamined. Here, we analyze continuous hour-long measurements of suspended sediment and grain size fractions collected using a LISST-SL in the sand bedded portion of the Fraser River, BC. Mean concentrations for suspended sediment and grain size fractions were computed over increasing time periods and compared to a long duration mean concentration to determine when a sample became representative. A cumulative probability distribution was generated for multiple iterations of this process. All suspended sediment load and grain size fractions bear a low probability of accurately representing the actual mean concentration over standard bottle sample durations. A probability >90% of accurately representing the mean of volumetric concentration requires 9.5 minutes of sampling.



**Keywords**: suspended sediment; point-integrated bottle sampling; LISST-SL

## Acknowledgements

I would like to thank my supervisory committee, Jeremy Venditti, Michael Church, and Ray Kostaschuk, for their guidance and feedback throughout this process. I would especially like to thank Jeremy and Mike for teaching me everything I know about fluvial geomorphology. Thank you also to my examining committee, Brian Menounos and Kirsten Zickfield for their additional insights and comments to improve my thesis.

I would like to thank Ray and Jeremy for their help during my fieldwork. I would also like to acknowledge funding from NSERC Discovery grants (Jeremy Venditti).

Special thank you to Ryan Bradley who has been a great friend and mentor and thanks to Dan Haught who taught me beer and MATLAB. Thank you to Krystyna Adams for her love and support and thank you to my family who has always been so encouraging.

# Table of Contents

Approval ..... ii
Abstract ..... iii
Acknowledgements ..... iv
Table of Contents ..... v
List of Tables ..... vii
List of Figures ..... viii

**1.0. Introduction ..... 1**

**2.0. Methods ..... 5**
2.1. Study Site ..... 5
2.2. Observations ..... 6
2.3. Data Analysis ..... 7

**3.0. Results ..... 13**
3.1. Variability in grain size and concentration ..... 13
3.2. Spectral Estimates ..... 15
3.3. Cumulative probability of NSMV method ..... 19
3.4. Temporary stabilization of $\beta$ ..... 21
3.4.1. Suspended sediment loads ..... 21
3.4.2. Grain size fractions ..... 24

**4.0. Discussion ..... 30**

**5.0. Conclusion ..... 33**

**References ..... 34**

Appendix A. Power spectral estimates of suspended sediment load ..... 38
Volumetric Concentration ..... 38
Silt load ..... 39
Washload ..... 41
Suspended bed material ..... 42
$D_{50}$ ..... 43
Appendix B. Persistent stabilization of $\beta$ ..... 44
Suspended sediment loads ..... 45
Grain size fractions ..... 46
Appendix C. Sampling time for a specified level of probability ..... 47
Suspended sediment loads ..... 47
Grain size fractions ..... 49

Appendix D. Point of diminishing returns ..... 51
Suspended sediment loads ..... 52
Grain size fractions ..... 52

# List of Tables

Table 3.1. Summary of the dominant periods underlying the downstream water velocity spectral signal. All values in the table are presented in seconds. ..... 18

Table 3.2. Time in seconds to achieve a specified level of probability of representing mean suspended sediment load concentration using temporary stabilization. Times were recorded from the cumulative probability curves of Sites 1 and 2. Each variable is depth averaged for the associated probability level. ..... 26

Table 3.3. Time in seconds to achieve a specified level of probability of representing grain size fraction using temporary stabilization. Times were recorded from the cumulative probability curves of Sites 1 and 2. Each variable is depth averaged for the associated probability level. ..... 28

# List of Figures


Figure 2.1. Grain size distribution captured by the LISST-SL a) before and b) after erroneous first 4 and last 2 bins were removed. Instantaneous concentrations for each grain size bin over a ten-minute period are presented. ..... 8

Figure 2.2. Example of non-stationary mean value for sand load at 0.6*h* of Site 2. The confidence bounds represent a range of mean values characteristic of the true mean value for a given sample size. As the incremental mean value $\beta$, increases in sample size it may become representative for a minimum of 60 seconds and be considered to stabilize temporarily. $\beta$ will also become representative for the duration of the measurement and may be considered to stabilize persistently. ..... 12

Figure 3.1. Representative time series at Site 2, 0.6*h* of a) volumetric concentration, silt load, washload, sand load, and suspended bed material and b) $D_{10}$, $D_{16}$, $D_{50}$, $D_{84}$, and $D_{90}$. ..... 14

Figure 3.2. Coefficient of variation for a) Sites 1 and b) 2 computed for each LISST-SL grain size bin. ..... 15

Figure 3.3. Spectral estimates of streamwise velocity from Sites 1 and 2 for 0.1*h*, 0.2*h*, 0.4*h*, 0.6*h*, 0.8*h*, and 0.9*h*. ..... 16

Figure 3.4. Examples of spectral estimates of suspended sediment concentration for various fractions at 0.6*h* of Site 2. ..... 17

Figure 3.5. Comparison between cumulative probability plots on the condition of (a) persistent stabilization and (b) temporary stabilization from 0.1*h* of Site 2. Results from (b) show a higher probability of a short duration sample approximating the long-term average than is observed in (a). ..... 20

Figure 3.6. Cumulative probability plots of suspended sediment loads with the condition of temporary stabilization of the $\beta$ signal. Measurements from Site 1 at a) 0.1*h*, b) 0.2*h*, c) 0.4*h*, d) 0.8*h*, and Site 2 at e) 0.1*h*, f) 0.2*h*, g) 0.4*h*, and h) 0.6*h* show the cumulative probability of obtaining a sample with a representative grain size moment value when measuring for a given period of time. ..... 23

Figure 3.7. Cumulative probability plots of grain size fractions with the condition of temporary stabilization of the $\beta$ signal. Measurements from Site 1 at a) 0.1*h*, b) 0.2*h*, c) 0.4*h*, d) 0.8*h*, and Site 2 at e) 0.1*h*, f) 0.2*h*, g) 0.4*h*, and h) 0.6*h* show the cumulative probability of obtaining a sample with a representative grain size moment value when measuring for a given period of time. ..... 25

# 1.0. Introduction

Fluvial sediment transport is a key component of the overall denudation of the continental surface [Milliman and Meade, 1983; Milliman and Syvitski, 1992]. Sediment in rivers may be transported either in suspension, as bedload, or in solution. The suspended load is comprised of materials supported by upward fluid stress sufficient to keep a particle from settling to the bed. The finest portion of the suspended load is the washload, which typically constitutes less than 10% of the bed material and is transported in near-continuous suspension [Church, 2006]. Bed material is coarser than washload but may also travel in suspension provided the upward directed fluid stresses are greater than the downward settling velocity of the sediment grains [Bridge, 2003]. Bedload comprises the coarsest particles, which move by rolling, sliding, or saltating along the bed. Globally, suspended sediment contributions to the oceans account for an estimated $16.2 \times 10^9$ tons annually while bedload is about $1.6 \times 10^9$ tons [Syvitski et al., 2005].

Suspended sediment concentrations are typically measured by collecting samples of water-sediment mixtures. Bottle samples are the traditional method for obtaining suspended sediment samples and may be collected using either depth- or point-integrated methods. Depth-integrated sampling involves lowering the sediment sampler from the river surface to the bed of the channel at a uniform rate while a bottle within the sampler collects an incremental volume of the water-sediment mixture from all points along the sampled depth. Each location chosen for a measurement is known as a sampling vertical and the movement of the sampler from the surface to the bed, or vice versa, is known as a transit. Point-integrated sampling involves lowering the sampler to a specific depth in the water column and collecting a volume of water-sediment mixture at a particular point in the flow [Tassone and Lapointe, 1999]. The number of point-integrated samples recommended for a channel >5m depth is 7: one measurement is made at the surface, another at the bed, and five more at 0.2*h,* 0.4*h*, 0.6*h*, 0.8*h*, and

0.9*h* where *h* is channel depth [Tassone and Lapointe, 1999]. This type of bottle sampling is designed to capture the mean suspended sediment concentration in the flow through time averaging.

Topping et al. [2011] identified four common sources of error arising from depth-integrated suspended sediment sampling: (1) bed contamination, (2) pressure-driven inrush, (3) inadequate number of sampling verticals collected across the channel width, and (4) inadequate time averaging. Error arising from (1) and (2) is the result of improper use of the suspended sediment sampler and can be easily rectified. Additional verticals across the channel will reduce uncertainty associated with (3) [Topping et al., 2011]. To address the uncertainty with inadequate time averaging Topping et al. [2011] recommended doubling the number of transits in standard two-way depth integrated sampling, which introduces minimal time averaging at all points of the depth. This method was found to reduce uncertainty by ~30% in each grain size class between multiple samples.

The error associated with point-integrated suspended sediment bottle sampling has not been addressed in the literature. It is reasonable to assume that point-integrated sampling is subject to the same user-induced errors, inadequate cross-section sampling and inadequate time averaging problems identified by Topping et al. [2011]. These sources of error can also be resolved in the same way, but it is not clear how many additional point-integrated samples need to be taken to obtain an accurate estimate of suspended sediment concentration. Indeed, the time required to obtain an accurate estimate of suspended sediment concentration in rivers is not known because the minimum time for a sample is set by the need to adequately average over variability in the flow. The maximum duration of bottle sampling is constrained by the volume of the bottle and flow velocity. If point-integrated sampling techniques are designed to represent the mean concentration in suspension [Tassone and Lapointe, 1999] then the sample duration of the bottle sampler must average enough variability in the flow to provide an accurate estimate of the mean. The accuracy of the sample relates to the closeness of the suspended sediment sample to the true underlying mean value. The true underlying mean value is affected by intermediate frequency variability in flow and sediment concentration on the order of minutes to possibly tens of minutes in duration.

The precision of the sample relates to the how closely multiple measurements of the mean concentration resemble each other. The precision of the sample is affected by high frequency variation in the suspended sediment concentration occurring over seconds to minutes. Repeated samples of suspended sediment are required to improve the accuracy of the measurements and to identify the appropriate sample period that will account for both intermediate and high frequency fluctuations in suspended sediment and fluid flow variability.

Variability in suspended sediment concentration is associated with variations in fluid velocity. Fluctuations in the downstream or cross-stream fluid velocity are the result of fluid flow events varying in magnitude and frequency. At the finest scales, variability in fluid flow is induced by turbulent fluctuations; at the largest scales, variability exists in climatic contributions to annual flow conditions. Between these two extremes of the fluid velocity spectrum exist coherent flow structures (CFS), which occupy all scales of turbulent fluid flow and contribute energy and momentum mixing to the transport of material in the flow. Low magnitude, high frequency near-wall CFS such as low-speed streaks [Kline et al, 1967], sweeps and ejections [Lapointe, 1992], and quasi-streamwise vortices [Adrian, 2013] occur in the near-wall portion of the inner layer [Adrian and Marusic, 2012]. Large-scale motions (LSM) of intermediate frequency such as kolks [Kostaschuk and Church, 1993] are upward sweeping fluid vortices that are also effective at entraining bed sediment into suspension. Large CFS features such as very large-scale motions (VLSM) occupy the entire water column and extend roughly 20 times the boundary layer thickness downstream [Hutchins and Marusic, 2007]. It remains unclear whether VLSM are discrete, random CFS features or if they are an amalgamation of LSM aligned in the streamwise direction [Adrian and Marusic, 2012; Marquis and Roy, 2013]. It is also unclear if VLSM actively erode and transport sediment or if the composite smaller motions perform this task [Adrian and Marusic, 2012].

Fluctuation in suspended sediment concentrations is related to availability of sediment and the incidence of shear stresses capable of entrainment. Higher concentrations of suspended sediment are strongly correlated with higher upward velocities capable of vertical mixing [Lapointe, 1992, 1996; Kostaschuk and Church 1993; Shugar et al., 2010; Bradley et al., 2013; Kwoll et al., 2014]. At the finest scales,

sweeps and ejections are brief events, lasting 3-8 seconds, which contribute the bulk majority of vertical sediment mixing [Lapointe, 1992]. In tidal rivers, contributions to net sediment flux over tidal cycles are dominant during low tide when mean flow velocities are highest [Kostaschuk and Best, 2005; Bradley et al., 2013; Kwoll et al., 2014]. Observations also indicate that, under decelerating flows resulting from rising tides, enhanced turbulence produces larger scale suspension events [Kostaschuk and Best, 2005], although the contribution to net sediment flux does not appear to be as great [Bradley et al., 2013; Kwoll et al., 2014].

The interaction of all sources of variability produces varying suspended sediment concentrations. Improving suspended sediment sampling techniques relies on understanding the contributing sources of variability and the frequency and magnitude with which they occur. By identifying the frequency of the dominant events influencing suspended sediment concentrations, the maximum time period over which the flow should be sampled can be established. An ideal record length balances the need to adequately capture high-frequency contributions to the downstream flow variability generated by interaction of the flow with the boundary without capturing externally forced low-frequency changes in flow lasting hours or longer (nival events, synoptic scale floods, tidal influences [e.g. Soulsby, 1980]). Here, we seek to establish the time required to collect a point-integrated sample of suspended sediment with a representative mean concentration. A representative mean concentration is the concentration of suspended sediment in flux after turbulence in the signal has been averaged out. Do current point-sample measurement techniques adequately capture mean concentration of suspended sediment? What sample duration is required to obtain an accurate mean concentration? Does the time required to obtain a representative mean concentration vary for different components of the suspended sediment load?

# 2.0. Methods

## 2.1. Study Site

Field measurements were conducted along a reach of the Fraser River at Mission, British Columbia, Canada, approximately 85 km upstream of the outlet of the river where it flows into the Strait of Georgia. Mission is 15 km downstream of the gravel-sand transition in the Fraser River, which is associated with a substantial break in water surface slope that delivers suspended sand to the bed [Venditti and Church, 2014]. The bed material at Mission is 0.38 mm sand forming small dune features over most of the bed during moderate to high flows.

Mean annual flow at Mission is 3410 $m^3$ $s^{-1}$ and the mean annual flood is 9790 $m^3$ $s^{-1}$ [McLean et al., 1999]. Major discharge events are dominated by the spring snowmelt beginning in April with peak discharges between May and July before discharge recedes through August and September [Venditti et al., 2014]. The Mission reach of the Fraser River experiences minor tidal effects during the freshet but no saltwater intrusion (see Dashtgard et al., 2012 for a recent review). This reach also has minimal boat traffic, allowing for long instrument deployments, and there has been a considerable number of previous works characterizing sediment transport in the reach [McLean et al., 1999; Domarad, 2011; Attard, 2012; Attard et al., 2014; Venditti and Church, 2014; Venditti et al., 2015].

Peaks in sediment transport precede annual peaks in flow discharge during freshets. On the basis of a sediment transport measurement program undertaken by the Water Survey of Canada between 1966 and 1986, McLean et al. [1999] reported the mean total suspended load is 17 $x10^6$ t $yr^{-1}$ of which, suspended clay (<1 $\mu$m) accounts for 2.3 $x10^6$ t $yr^{-1}$, silt load (<64 $\mu$m) is 8.3 $x10^6$ t $yr^{-1}$, and sand load (>64 $\mu$m) is 6.1 $x10^6$ t $yr^{-1}$. The nominal division between washload and bed material load at Mission is 0.18

mm [McLean et al., 1999; Attard et al., 2014]. The washload comprises the vast majority of the total suspended load, accounting for 14 $x10^6$ t $yr^{-1}$. The remaining 18% of total suspended load is the suspended bed-material load. The annual bedload is estimated to be 1.5 $x10^5$ t $yr^{-1}$ [McLean et al., 1999].

## 2.2. Observations

Continuous records of suspended sediment concentration were collected from May 30 to June 2, 2013 using a Sequoia LISST-SL (laser in-situ scattering transmissometer), a streamlined instrument with stabilizing fins that uses laser diffraction to sample instantaneous volumetric particle concentration, grain-size distribution, downstream water velocity, optical transmission, depth, and water temperature information at 0.5 Hz [Sequoia Scientific, 2012]. Data were recorded in 32 log-spaced bins ranging from 1.90 to 381 μm. The instrument isokinetically pumps water through a front nozzle and into a laser detection chamber. The pump is dynamically adjusted to match water velocity at the instrument nose measured using a pitot tube. Data were recorded in a topside control box for post-processing. No physical samples of suspended sediment were collected. We made no attempt to compare the LISST-SL concentrations and grain-size to conventional bottle samples because we are interested in the variability of the signal and not the absolute values of any variable.

Suspended sediment concentration data were measured from a 6 m boat. Average discharge over this period was 8265 $m^3$ $s^{-1}$, just below the mean annual peak flow. The LISST-SL was deployed from the side of the boat with a USGS B-reel operated through a davit to allow measurement at desired depths. Slight modifications to the Water Survey of Canada's sampling program were made to ensure optimal use of the sediment sampler. Instead of a measurement collected at the surface, a measurement was made at 0.1*h* to ensure the sampler remained submerged for the entire duration. Samples were not collected close to the bed to avoid potential instrument clogging with coarse sediment and contact with the bed. As a result 6 points in the water column were measured, each for 1 hour: 0.1*h*, 0.2*h*, 0.4*h*, 0.6*h*, 0.8*h*, and 0.9*h*. Vertical position was measured with an onboard pressure sensor. Spatial coordinates were recorded using differential GPS. Two locations were selected near

Mission, B.C; Site 1 is located at 49°07’39” N, 122°17’50” W and Site 2 is located 0.2 km upstream at 49°07’42” N, 122°17’41” W. The bed at both locations is approximately flat with small dune features rising on average 10 cm from the bed. Bed material samples were collected at both locations by dredging a portion of the bed with a grab sampler.

## 2.3. Data Analysis

Data from the LISST-SL topside control box were processed using MATLAB code that employed Sequoia’s irregular shaped particle model to calculate total volumetric, silt (<64 μm), sand (>64 μm), washload (<177 μm) and suspended bed material (>177 μm) concentrations as well as grain size fractions. Inspection of the empirically derived frequency curves of the collected data indicated a spike in concentration in the first four and last two grain-size bin classes measured by the LISST-SL. Grain sizes between 1.90 – 3.69 μm and 273 – 381 μm are at the edge of the laser detector and are most susceptible to errors if the laser alignment is not perfect (See Domarad, 2011). These grain-size bins were removed from subsequent analysis so that the measured range of suspended sediment is 3.69-273 μm (Figure 2.1). To determine the effect of this truncation, a comparison of the grain size distribution to a cumulative distribution of suspended sediment collected during freshet at Mission in 1974 and an image analysis of physical samples of suspended sediment collected in 2015 was performed. The comparison indicates ~15% of the coarsest portion of the grain size distribution is not measured with the 273 μm cut off. Additionally we explored the variability in volumetric concentration in each grain-size bin by calculating the coefficient of variation, which is the standardized measure of dispersion of a probability distribution, defined as the ratio of the standard deviation $\sigma$, to the mean $\mu$.

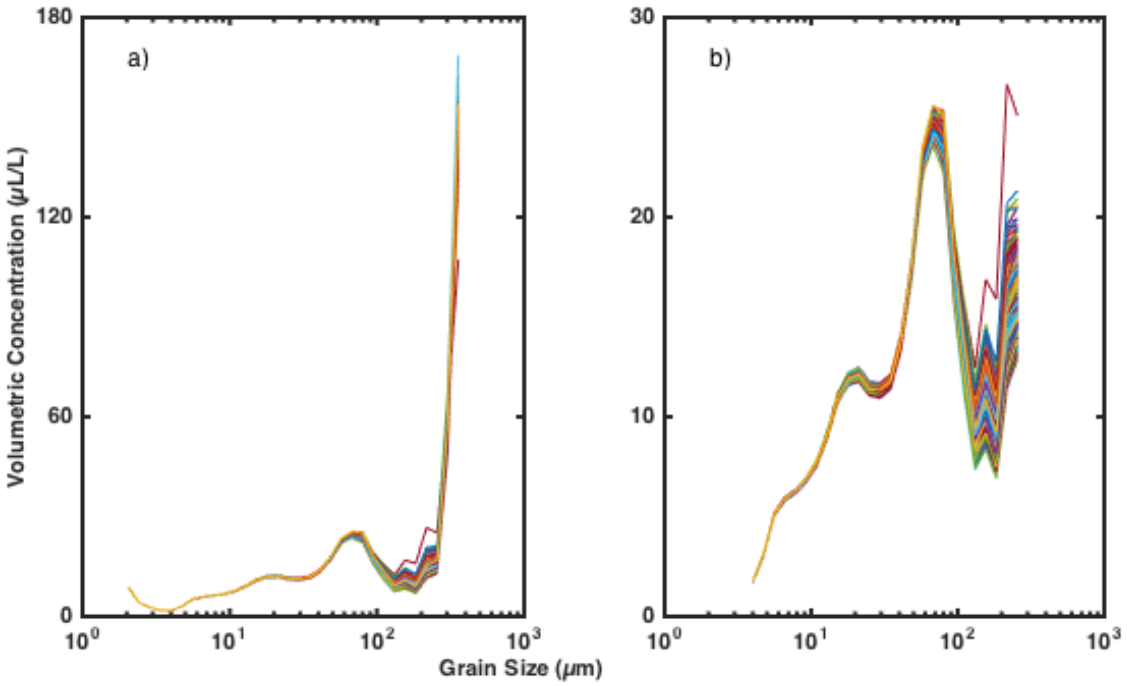


**Figure 2.1. Grain size distribution captured by the LISST-SL a) before and b) after erroneous first 4 and last 2 bins were removed. Instantaneous concentrations for each grain size bin over a ten-minute period are presented.**

We are interested in capturing all variability that exists between turbulence scales and mean flow variation that is set by the freshet hydrograph and tidal influences. The minimum scale of interest is set by the sampling frequency of the LISST-SL at 0.5 Hz. The maximum scale of interest was established using univariate spectral analysis on time series at both field sites. Effects of tidal drift were removed through a linear detrending of each of the 1-hour time series.

Instrument clogging and low water velocities at 0.8*h* and 0.9*h* of the profile at Site 2 resulted in highly fragmented suspended sediment concentration signals and consequently are omitted from further consideration. Water velocities at 0.9*h* at Site 1 were lower than minimum LISST-SL requirements for isokinetic sampling so the rate of suspended sediment intake was occasionally greater than would be expected under isokinetic conditions.

An attempt was made to use distributions of the mean concentration for all time series data to quantify the error associated with increasing the averaging time of a sample. The expectation was that as the size of the averaging window increased, the error associated with the increasing time window would decrease to some constant value. However, as the time window increased the number of samples obtained over the finite length of time series decreased. The distributions of the subsampled signal were also non-normal according to Kolmogorov-Smirnoff and Shaprio-Wilk normality tests ($a$ = 0.1). The combination of decreasing population size and non-normal distributions preclude a simple error assessment.

An alternative approach to identifying a representative mean value employing a probability-based method was conceived. The probability method involved determining the time required to collect a sample mean value that had a concentration representative of the true mean value. The true mean value was associated with a concentration signal of specific length chosen based on some underlying intermediate-frequency trend in the data.

Spectral analysis of the streamwise water velocity and suspended sediment concentration signal was used to establish the intermediate frequency cut off for the analysis. The time series signal at each flow depth was detrended and the average of three spectral estimates was used to produce a time invariant spectral estimate [Schmid, 2012]. Each segment length was equal to $2^m$ where $m$ was chosen to sample the greatest length of the available signal. There is a 50% overlap between successive signal segment pairs so that segment 1 and segment 3 does not sample the same portions of the time series and segment 2 samples half of the first and last segments. Spectral estimates were calculated between 0 Hz and the Nyquist frequency (0.25 Hz), at intervals of $\frac{1}{nT_s}$ where $n$ is the signal segment length and $T_s$ is sampling period. A Hamming window of length equal to that of the signal segment modified each time series before processing by the Welch method [Schmid, 2012]. The significance of each peak in the spectral estimate was determined by normalizing the Fourier coefficients to convert the power spectral density estimate to a Chi-square cumulative distribution function with 2 degrees of freedom [Menke and Menke, 2012]. Spectral peaks were compared against all other calculated frequencies between 0 and 0.25 Hz to ensure the

peak was a significant component of the spectral estimate. A dominant peak was identified as the maximum scale of interest, herein termed the measurement duration. The measurement duration must be of adequate length to minimize errors due to the loss of low to intermediate frequency contributions and short enough to reduce errors associated with non-stationarity in the signal caused by changing tidal conditions [Soulsby, 1980].

The minimum time period required to obtain a representative sample of suspended sediment was determined using the Non-Stationary Mean Value (NSMV) Technique [Bendat and Piersol, 1966]. Suspended sediment concentration is a non-stationary process dictated by changes in discharge associated with the freshet hydrograph, tides, and sediment supply. The NSMV Technique enables the prediction of a range of mean value estimates for any time period with the knowledge of the signal's mean value and standard deviation. The ratio of the signal's true mean value $\mu_x(t)$, to that of the sample mean value $\hat{\mu}_x(t)$, indicates the equivalence of the sample mean value to the signal's true mean value. Confidence bounds are produced for a distribution of possible mean values using

$$\frac{\mu_x(t)}{\hat{\mu}_x(t)} = \left(1 \mp c\left[\frac{\sigma_x(t)}{\sqrt{N}\mu_x(t)}\right]\right)^{-1} \quad (1)$$

where $\sigma_x(t)$ is the standard deviation of the signal, *N* is sample size, and *c* is a constant indicating the type of distribution and the degree of certainty in the confidence interval. As *N* increases the probability of the sample mean resembling the true mean increases greatly, regardless of the magnitude of the standard deviation and underlying distribution [Bendat and Piersol, 1966].

The entire length of the suspended sediment concentration record was utilized in evaluating the non-stationary mean. A subsampled segment equal in length to the measurement duration was extracted and processed to determine the time required to obtain a representative mean value. A mean value for each subsampled signal segment was computed over an increasing sample size producing a signal of incremental mean concentration. The incremental mean value signal was then divided by the true mean value of the signal. The true mean value was established by calculating the mean

concentration of the measurement duration and subsequent sample mean values were compared to this value. The resultant signal, β, was then compared to the confidence bounds produced by Equation 1 and the point was recorded at which the incremental sample mean value became representative of the true mean value with 95% confidence (Figure 2.2). The result of multiple iterations of this process produced a distribution of minimum time periods required to obtain a sample mean concentration representative of the true mean concentration for each component of the suspended sediment load. The distribution of times was converted to a cumulative probability plot indicating the likelihood of obtaining a sample mean concentration representative of the true mean concentration for a given time period. Two sets of results were collected using the NSMV Technique. One method required persistent stabilization of the β signal on the long-term average; the point at which a sample became representative was recorded only if the remainder of the β signal remained representative. The second set of results was recorded under the condition of temporary stabilization. Temporary stabilization of the β signal occurs at the first instance where β becomes representative for minimum of 60 seconds; the point at which this occurs is the recommended sampling period (See Figure 2.2). The 60-second period ensured that the β signal closely approximated the long-term value for a brief period of time and did not vary too greatly over the course of a short-term measurement.

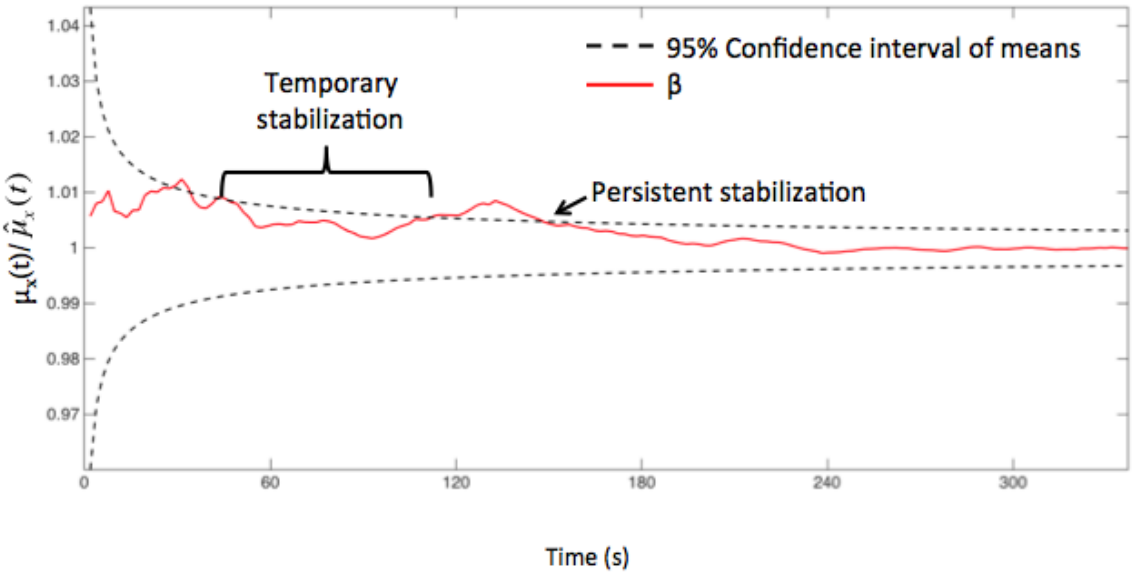


**Figure 2.2.** **Example of non-stationary mean value for sand load at 0.6*h* of Site 2. The confidence bounds represent a range of mean values characteristic of the true mean value for a given sample size. As the incremental mean value β, increases in sample size it may become representative for a minimum of 60 seconds and be considered to stabilize temporarily. β will also become representative for the duration of the measurement and may be considered to stabilize persistently.**

# 3.0. Results

## 3.1. Variability in grain size and concentration

Representative measurements of suspended sediment loads at 0.6*h* of Site 2 are presented in Figure 3.1a. Volumetric concentration of suspended sediment was calculated by summing the concentration of all measured grain size bins. Fractional sediment loads were calculated for silt load, sand load, washload, and suspended bed material based on classification criteria outlined above (See 2.1 Study Site). Sand load and suspended bed material have the greatest variability; silt load and washload have comparably lower variability because silt concentrations are well mixed within the water column. Much of the variability in the volumetric concentration is derived from variability in the sand load, which is suspended from the bed.

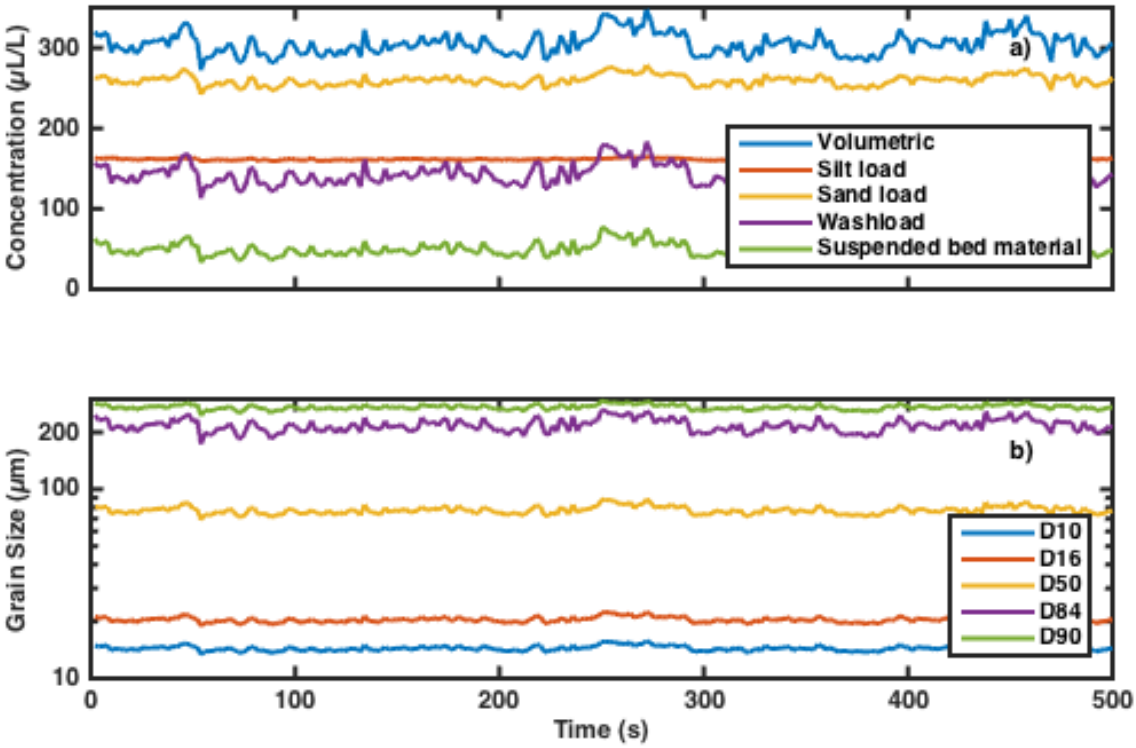


**Figure 3.1. Representative time series at Site 2, 0.6*h* of a) volumetric concentration, silt load, washload, sand load, and suspended bed material and b) $D_{10}$, $D_{16}$, $D_{50}$, $D_{84}$, and $D_{90}$.**

Grain size fractions $D_{10}$, $D_{16}$, $D_{50}$, $D_{84}$, and $D_{90}$ were calculated at each measured flow depth for both sites. A representative set of grain size fractions from 0.6*h* of Site 2 is presented in Figure 3.1b. $D_{84}$ has the greatest variability because it represents the behaviour of the sand load. $D_{90}$ has comparatively less variability because it is constrained by the edge of the grain size detector; the largest measured grain size cannot be larger than 273 µm. $D_{10}$ and $D_{16}$ also have less variability because they are strongly influenced by the lack of variability in the silt load. The coefficient of variation (CV), represented as a percentage (Figure 3.2) indicates a similar pattern of variability for both sites with increasing grain size for each measured depth. CV increases with grain size for all sizes except bed-material size particles representing the $D_{90}$ grain size fraction.

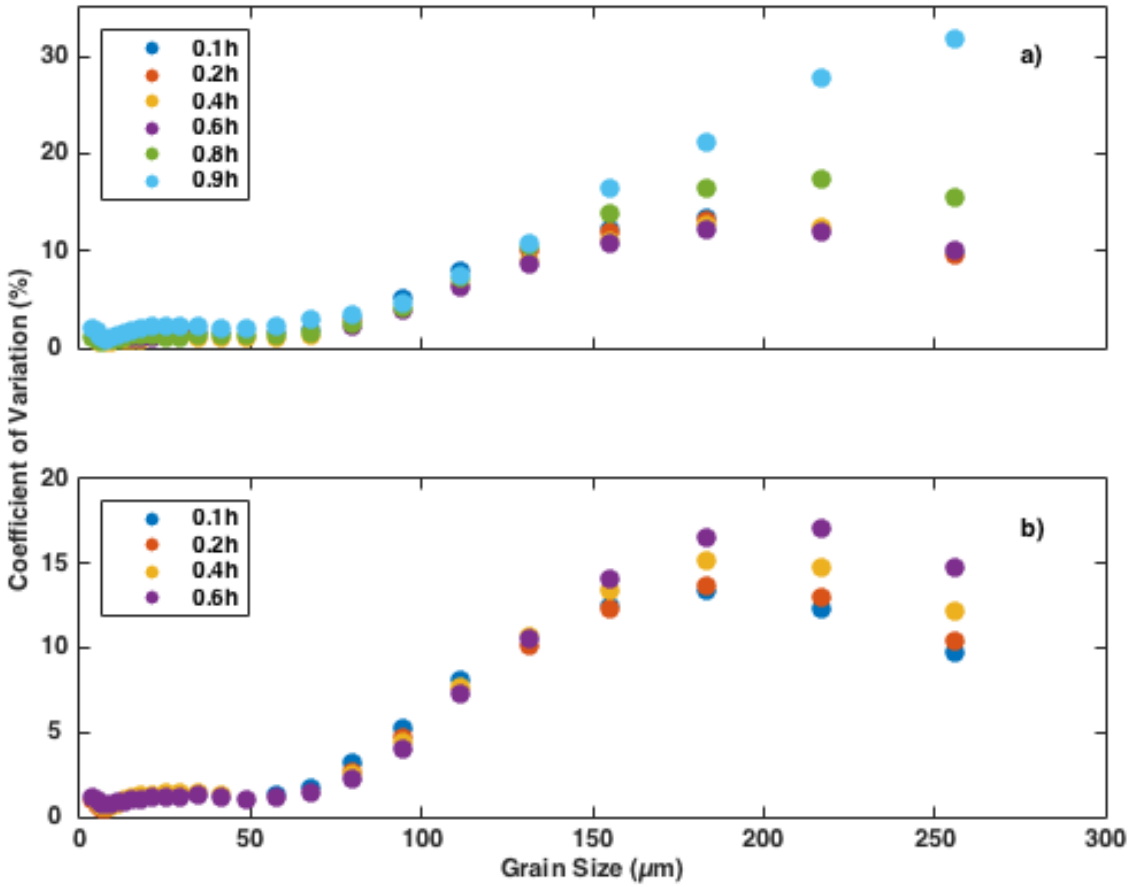


**Figure 3.2. Coefficient of variation for a) Sites 1 and b) 2 computed for each LISST-SL grain size bin.**

## 3.2. Spectral Estimates

Spectral analysis was performed on all silt load, sand load, washload, suspended bed material load, volumetric concentration, $D_{50}$ (see Appendix A) and streamwise water velocity signals. Peaks in the spectra were considered statistically significantly different from all other frequencies when a 90% confidence interval was exceeded. Intermediate frequency oscillations in downstream fluid velocity were present at the surface with increasing frequency towards the channel bed. The fluid velocity spectra performed at each measured depth along the sampling profile are presented for Sites 1 and 2 in Figure 3.3 and observed peaks summarized in Table 3.1. Spectral results of the suspended sediment load and grain size fractions are presented in Figure 3.4.

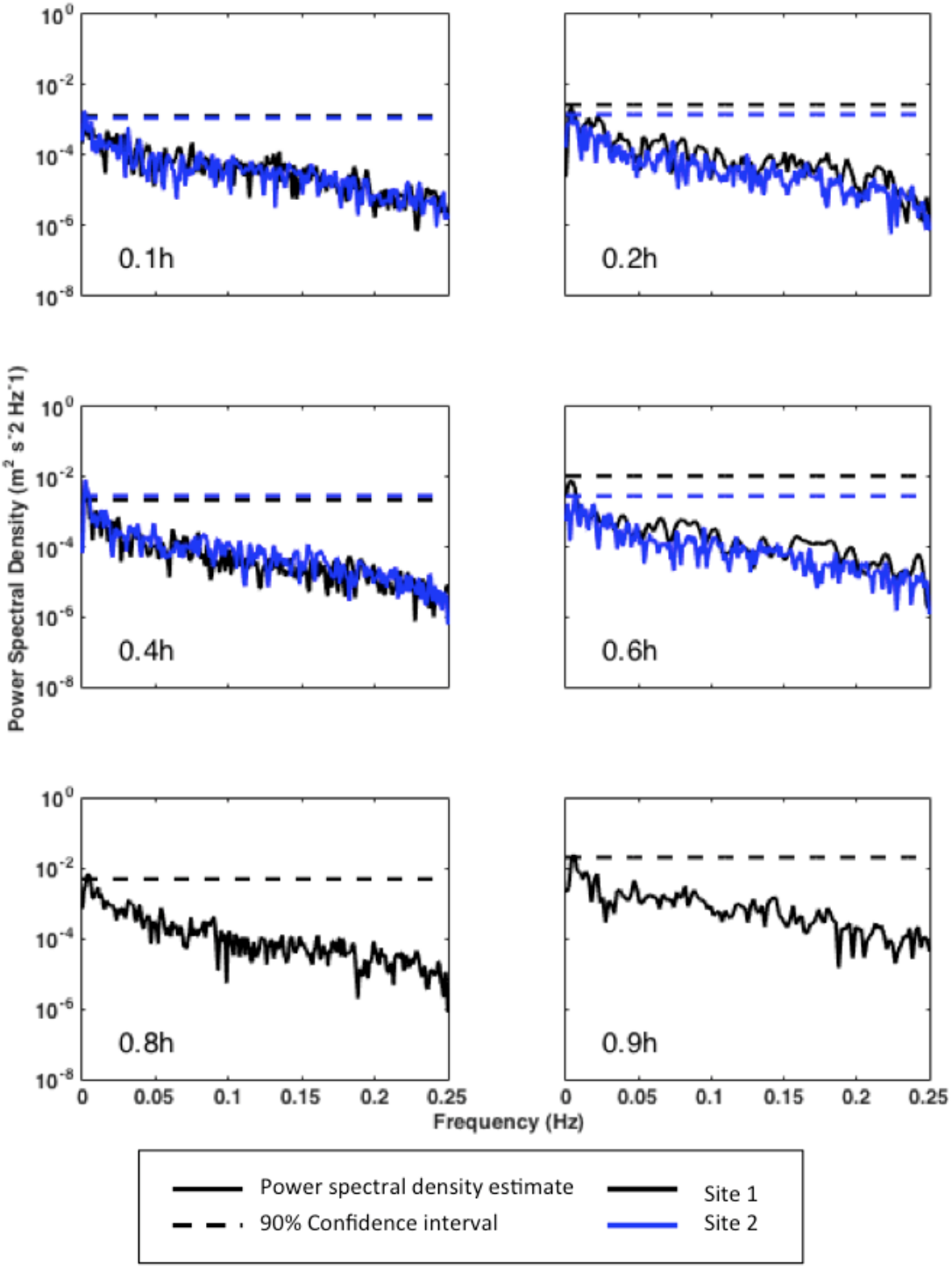


**Figure 3.3. Spectral estimates of streamwise velocity from Sites 1 and 2 for 0.1*h*, 0.2*h*, 0.4*h*, 0.6*h*, 0.8*h*, and 0.9*h*.**

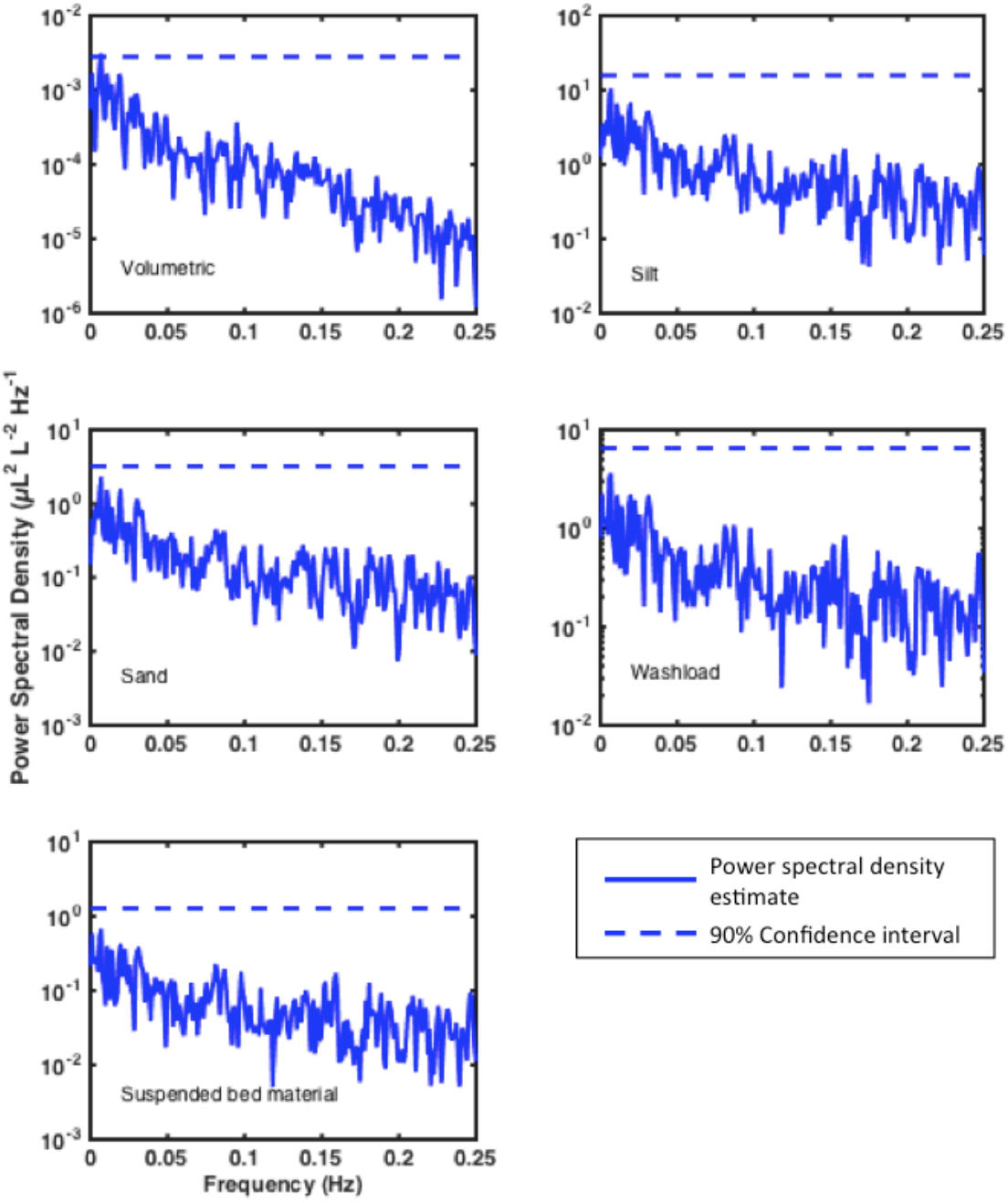


**Figure 3.4. Examples of spectral estimates of suspended sediment concentration for various fractions at 0.6*h* of Site 2.**

**Table 3.1. Summary of the dominant periods underlying the downstream water velocity spectral signal. All values in the table are presented in seconds.**

| | **0.1*h*** | **0.2*h*** | **0.4*h*** | **0.6*h*** | **0.8*h*** | **0.9*h*** |
|---|---|---|---|---|---|---|
| **Site 1** | 1024 | None | 512 | None | 256 | 256 |
| **Site 2** | 1024 | 256 | 512 | 146 | N/A | N/A |

Comparison of spectra shown in Figures 3.3 and 3.4 reveal that all measured spectra display variation in all frequencies with no clearly dominant peak and a continuous decrease in spectral power as frequency increases. The spectra exhibit Red noise tendencies common in turbulent flow conditions. Long period structures dominate in wake stretching and non-uniform decelerating fluids and contain a large proportion of turbulent energy resulting in spectral energies increasing as frequency decreases [Gray et al., 2005]. Red noise in the spectrum would include an increase in signal variability up to secular scales (tidal; synoptic) and so the observed peaks may not be a truly significant component of the time series.

Of the observed peaks in the streamwise velocity spectra the lowest frequency peak had a period of 1024 seconds, or 17.1 minutes. This period may be part of a Red noise spectrum and therefore not a true dominant spectral peak, but it is sufficiently long to incorporate previously identified observed dominant flow oscillations. Lapointe [1993] observed flow oscillations ranging between 1 and 13.6 minutes, and contributing approximately 30% of the vertical sand flux. Establishing the upper limit of the NSMV measurement period at 17.1 minutes incorporates the upper limit of Lapointe's findings and occurs at a natural break in spectral frequencies, $2^{10}$. This measurement period for the NSMV analysis is sufficiently long to capture 13.6-minute flow oscillations as well as potentially longer period oscillations contributing to suspended sediment flux. While higher frequencies were present lower in the flow depth, suggesting dominance of bed generated turbulence or CFS, the use of a single intermediate frequency limit allows for comparability between NSMV results at all flow depths.

## 3.3. Cumulative probability of NSMV method

Two versions of the NSMV method applied to the suspended sediment and grain size fraction data from both sites show the cumulative probability of persistent and temporary stabilization of the incremental mean value, $\beta$ (Figure 3.5). For suspended sediment loads $\beta$ represents the cumulative mean concentration, for grain size fractions, the average value of a particular grain size fraction. As $\beta$ increases in sample size the value stabilizes on a range of representative mean values within the 95% confidence interval of the long-term value. $\beta$ is considered to be representative, either temporarily or persistently, in its relation to the long-term average of the 17.1-minute measurement period and as such, can only be considered representative after the measurement period has been analyzed. This measurement period is only a subset of the changing flow conditions and variable suspended sediment conditions expected over tens of minutes to hours, much like a bottle sample is a subset of the 17.1-minute measurement period. The selected measurement period is sufficiently long to average out the short term fluctuations in sediment concentration and is great enough to capture the longest of the non-secular flow oscillations identified by Lapointe [1993], thus capturing the average concentration over an intermediate frequency flow oscillation and ignoring effects of secular changes. Since a sample was considered representative in relation to the long duration measurement period, the concentration of one stable representative sample may differ from that of another due to variations in mean and standard deviation of their respective measurement period. However, in both cases a sample mean is considered to be representative based on the population distribution of each respective measurement period. Since the entire length of the time series was used, a reasonable estimate of how likely a sample of given length is to be considered representative can be determined using a cumulative probability plot.

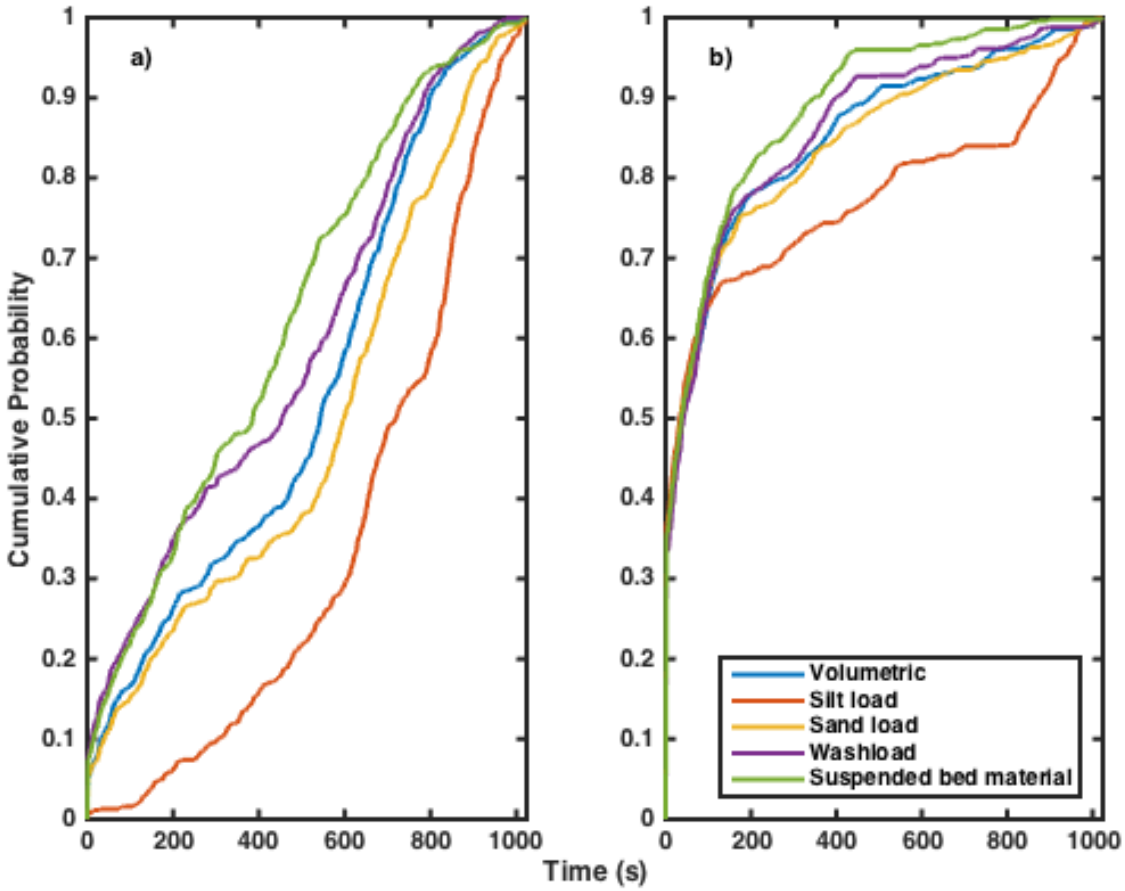


**Figure 3.5. Comparison between cumulative probability plots on the condition of (a) persistent stabilization and (b) temporary stabilization from 0.1*h* of Site 2. Results from (b) show a higher probability of a short duration sample approximating the long-term average than is observed in (a).**

An example of the results from the first set of structured observations requiring persistent stabilization are presented in Figure 3.5a where a sample was not considered to be representative of the long term value until $\beta$ had stabilized within the confidence range and remained representative for the duration of the measurement. An example of results from the second set of structured observations is presented in Figure 3.5b where the signal was accepted as representative after $\beta$ became representative for a minimum of 60 seconds. In both cases the point at which $\beta$ first becomes representative was recorded as the time required to obtain a representative sample.

Persistent stabilization of β requires more time to achieve the same level of probability compared with temporary stabilization (Figure 3.5). Persistent stabilization of β requires the signal to remain representative for the entire duration of the measurement and Figure 3.5a shows this requirement is unduly strict. Results show that the probability of persistent stabilization increases over the whole duration of the sample so that the longer a sample is measured the more likely it is to represent the long-term value. This method reveals that the probability of obtaining a representative value is dependent on the length of the sample, which is not a realistic scenario. It may also be an artifact of the underlying Red noise observed in the spectrum. This approach minimizes the possibility that short-term measurements may in fact represent the long-term average. Variability in the suspended sediment concentration and grain size fractions may push β out of the 95% confidence interval even if it had been considered representative for a substantial period of time. As a result, requirement of persistent stabilization of β presupposes highly probable samples will only be obtained by measuring approximately as long as the measurement duration

In contrast, temporary stabilization considers whether a shorter duration sample may accurately reflect the long-term mean, regardless of turbulence after the short duration sample is collected. This approach shows the probability that a sample collected by traditional means will accurately reflect the long-term value of interest so here we focus on temporary stabilization of β analysis. Cumulative probability results under persistent stabilization are presented in Appendix B.

## 3.4. Temporary stabilization of β

### 3.4.1. Suspended sediment loads

Analysis of the suspended sediment loads with temporary stabilization of the NSMV yields high probabilities of achieving a stable mean value for shorter measurement time periods. Cumulative probability plots for suspended sediment loads of Sites 1 and 2 are presented in Figure 3.6. A short file at 0.6*h* and non-isokinetically collected data at 0.9*h* of Site 1 obscure trends observed at other measurement depths

and were removed from consideration. Silt load was also removed from analysis of 0.6 *h* at Site 2 as it was deemed to be an outlier. At all depths there is 28 % probability of an instantaneous sample collected over 2 seconds accurately representing the long-term concentration. Short-term measurements up to 2-3 minutes show a rapid increase in probability with measurement time for most measured depths. The increase in probability in the initial minutes is approximately consistent for all variables such that there is no great difference in achieving stable value of one variable over another. Occasionally the silt load has lower probability than other variables for the same time period (Figure 3.6b, c, e). Beyond the initial increase in probability there is a decrease in the rate of improved probability with measurement time. The break in this trend is sometimes pronounced (e.g. Figure 3.6e) and sometimes gradual (e.g. Figure 3.6g). The break appears before 8 minutes, after which the slope of probability increase with time is greatly reduced.

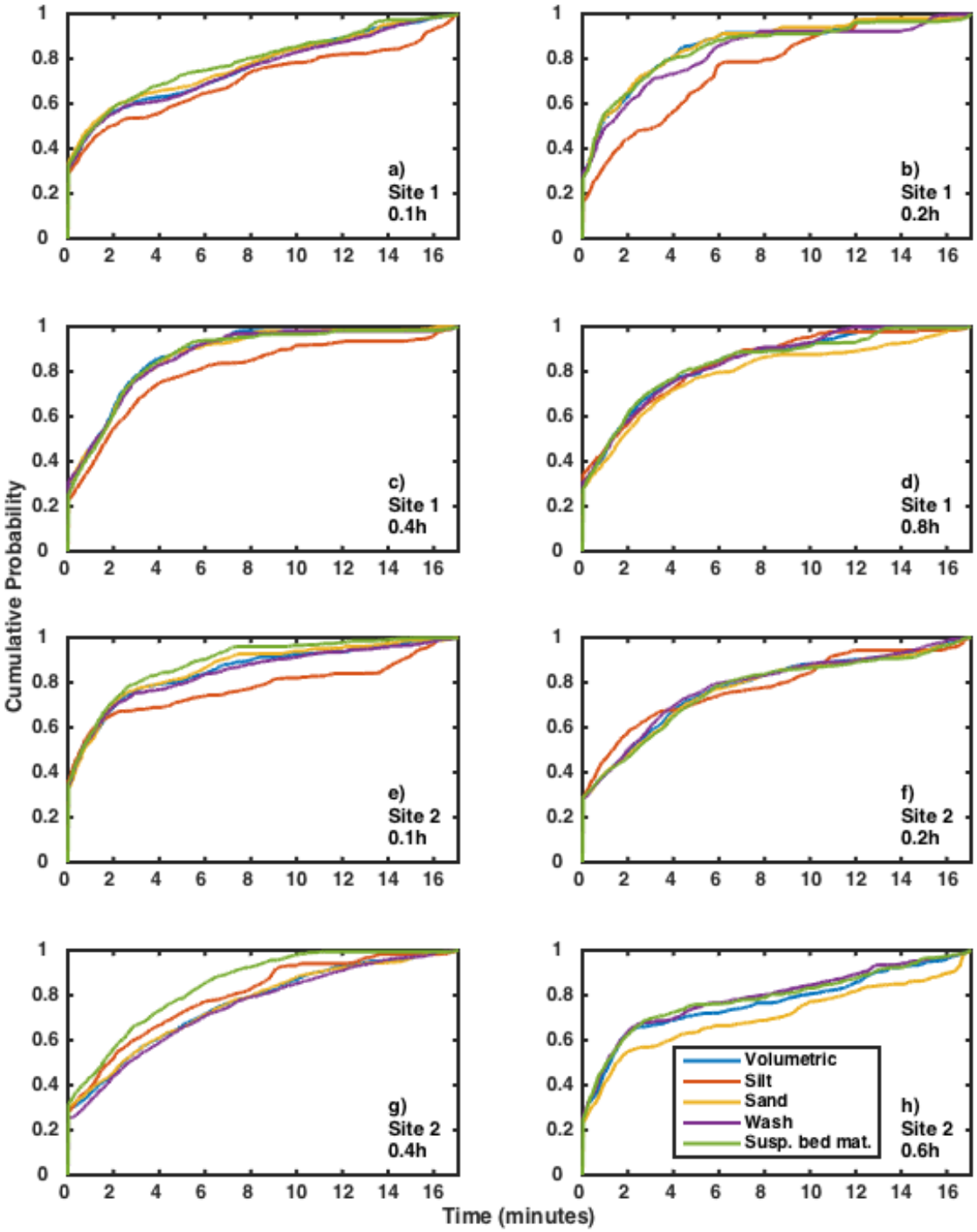


**Figure 3.6.** **Cumulative probability plots of suspended sediment loads with the condition of temporary stabilization of the β signal. Measurements from Site 1 at a) 0.1*h*, b) 0.2*h*, c) 0.4*h*, d) 0.8*h*, and Site 2 at e) 0.1*h*, f) 0.2*h*, g) 0.4*h*, and h) 0.6*h* show the cumulative probability of obtaining a sample with a representative grain size moment value when measuring for a given period of time.**

### 3.4.2. Grain size fractions

Similar results are observed in the grain size fraction analysis of the NSMV presented in Figure 3.7 for Sites 1 and 2. Also similar to the previous set of results is that 0.6*h* and 0.9*h* were omitted from further consideration. Instantaneous samples indicate an 18 – 38 % probability of obtaining a representative value in 2 seconds of sampling, after which there is a rapid increase in the probability. The increase in probability is followed by a transition to lower rates of probability increase with time. The transition occurs, again, between ~2 and 8 minutes. Even more so than for suspended sediment loads, grain size fractions at all depths typically achieve an approximately similar level of probability in representing the long-term value at about the same measurement time.

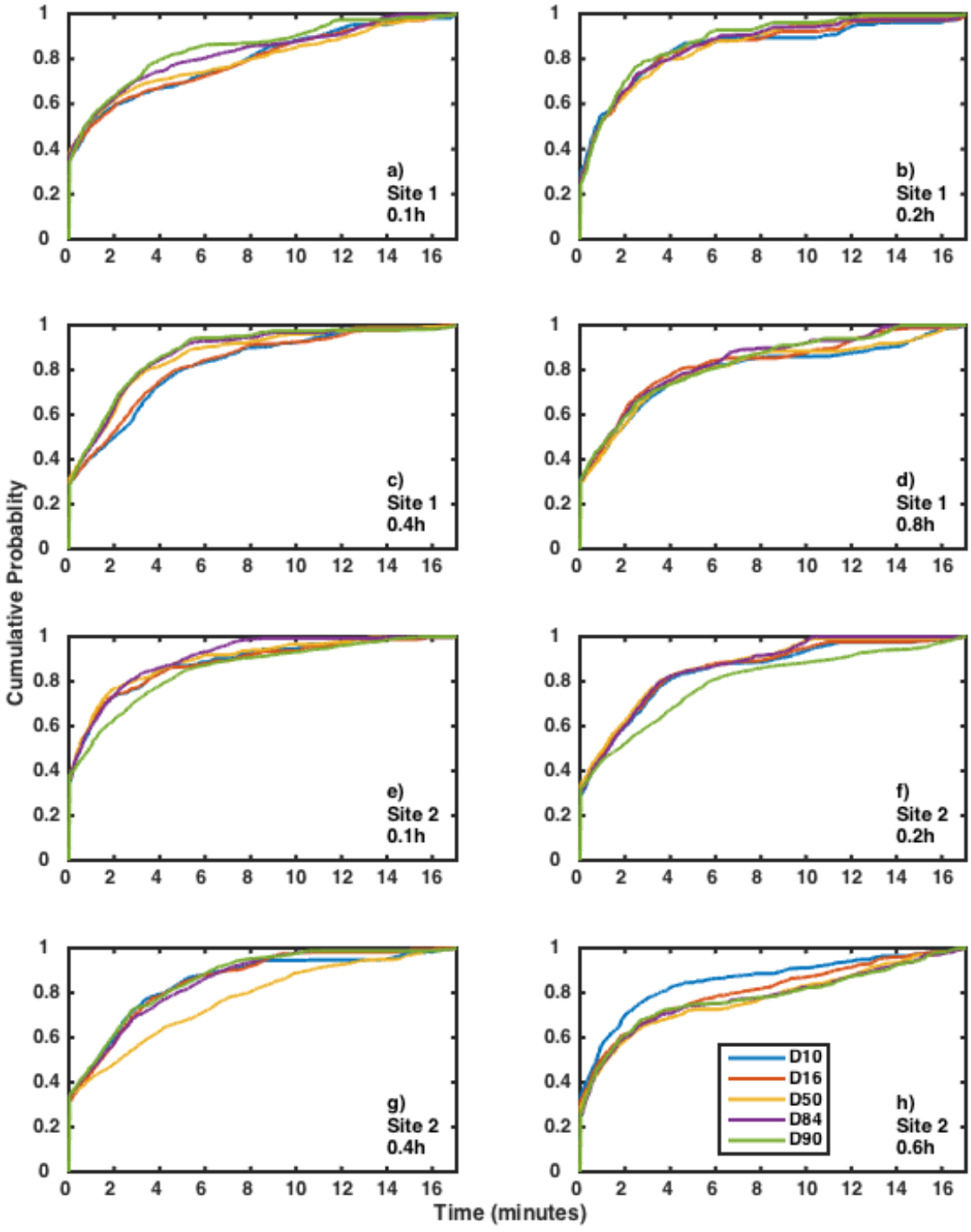


**Figure 3.7.** **Cumulative probability plots of grain size fractions with the condition of temporary stabilization of the β signal. Measurements from Site 1 at a) 0.1*h*, b) 0.2*h*, c) 0.4*h*, d) 0.8*h*, and Site 2 at e) 0.1*h*, f) 0.2*h*, g) 0.4*h*, and h) 0.6*h* show the cumulative probability of obtaining a sample with a representative grain size moment value when measuring for a given period of time.**

Look-up tables providing the time required to collect a sample of suspended sediment concentration or grain size fraction for a specified level of probability are provided for temporary stabilization of the mean value of suspended sediment loads (Table 3.2) and grain size fractions (Table 3.3) at Sites 1 and 2. Corresponding tables for persistent stabilization of the mean value for suspended sediment loads and grain size fractions at Site 1 and 2 appear in Appendix C.

**Table 3.2. Time in seconds to achieve a specified level of probability of representing mean suspended sediment load concentration using temporary stabilization. Times were recorded from the cumulative probability curves of Sites 1 and 2. Each variable is depth averaged for the associated probability level.**

| h | 50% | | 75% | | 80% | | 85% | | 90% | | 95% | | 99% | |
|---|---|---|---|---|---|---|---|---|---|---|---|---|---|---|
| | Site 1 | Site 2 | Site 1 | Site 2 | Site 1 | Site 2 | Site 1 | Site 2 | Site 1 | Site 2 | Site 1 | Site 2 | Site 1 | Site 2 |
| VOLUMETRIC CONCENTRATION | | | | | | | | | | | | | | |
| 0.1 | 76 | 40 | 460 | 166 | 524 | 280 | 610 | 376 | 744 | 478 | 854 | 756 | 988 | 994 |
| 0.2 | 48 | 126 | 186 | 322 | 236 | 418 | 266 | 510 | 358 | 708 | 710 | 916 | 1018 | 1000 |
| 0.4 | 78 | 146 | 162 | 396 | 194 | 492 | 230 | 570 | 306 | 648 | 418 | 792 | 1010 | 966 |
| 0.6 | -- | 74 | -- | 438 | -- | 578 | -- | 712 | -- | 770 | -- | 918 | -- | 1010 |
| 0.8 | 80 | -- | 234 | -- | 314 | -- | 360 | -- | 550 | -- | 668 | -- | 758 | -- |
| Avg. | 84 | | 296 | | 380 | | 454 | | 570 | | 754 | | 968 | |
| SILT LOAD | | | | | | | | | | | | | | |
| 0.1 | 112 | 34 | 500 | 416 | 654 | 530 | 878 | 824 | 934 | 876 | 988 | 928 | 1014 | 982 |
| 0.2 | 196 | 82 | 352 | 374 | 504 | 532 | 548 | 608 | 612 | 646 | 720 | 958 | 1010 | 1008 |
| 0.4 | 104 | 110 | 242 | 332 | 328 | 430 | 484 | 506 | 586 | 540 | 948 | 760 | 1008 | 1002 |
| 0.6 | -- | -- | -- | -- | -- | -- | -- | -- | -- | -- | -- | -- | -- | -- |
| 0.8 | 82 | -- | 260 | -- | 296 | -- | 378 | -- | 460 | -- | 582 | -- | 1008 | -- |
| Avg. | 103 | | 354 | | 468 | | 604 | | 665 | | 841 | | 1005 | |
| SAND LOAD | | | | | | | | | | | | | | |
| 0.1 | 60 | 42 | 442 | 152 | 514 | 248 | 614 | 344 | 746 | 400 | 834 | 648 | 1002 | 994 |
| 0.2 | 48 | 136 | 188 | 322 | 236 | 426 | 294 | 506 | 356 | 730 | 700 | 920 | 1018 | 1004 |
| 0.4 | 82 | 142 | 168 | 404 | 206 | 482 | 256 | 558 | 320 | 648 | 466 | 876 | 944 | 966 |
| 0.6 | -- | 66 | -- | 314 | -- | 468 | -- | 618 | -- | 736 | -- | 866 | -- | 1012 |
| 0.8 | 102 | -- | 278 | -- | 394 | -- | 450 | -- | 760 | -- | 900 | -- | 994 | -- |
| Avg. | 85 | | 284 | | 372 | | 455 | | 587 | | 776 | | 992 | |

| h | 50% | | 75% | | 80% | | 85% | | 90% | | 95% | | 99% | |
|---|---|---|---|---|---|---|---|---|---|---|---|---|---|---|
| | Site 1 | Site 2 | Site 1 | Site 2 | Site 1 | Site 2 | Site 1 | Site 2 | Site 1 | Site 2 | Site 1 | Site 2 | Site 1 | Site 2 |
| WASHLOAD | | | | | | | | | | | | | | |
| 0.1 | 72 | 38 | 452 | 174 | 546 | 312 | 648 | 404 | 784 | 538 | 868 | 802 | 980 | 980 |
| 0.2 | 64 | 122 | 276 | 302 | 328 | 370 | 350 | 532 | 448 | 728 | 892 | 888 | 934 | 968 |
| 0.4 | 76 | 158 | 170 | 426 | 212 | 506 | 274 | 600 | 326 | 696 | 410 | 818 | 1008 | 970 |
| 0.6 | -- | 90 | -- | 576 | -- | 688 | -- | 852 | -- | 968 | -- | 1000 | -- | 1016 |
| 0.8 | 80 | -- | 236 | -- | 310 | -- | 384 | -- | 458 | -- | 630 | -- | 698 | -- |
| Avg. | 88 | | 327 | | 409 | | 506 | | 618 | | 789 | | 944 | |
| SUSPENDED BED MATERIAL | | | | | | | | | | | | | | |
| 0.1 | 70 | 38 | 366 | 142 | 472 | 186 | 588 | 276 | 734 | 346 | 798 | 424 | 996 | 840 |
| 0.2 | 46 | 144 | 190 | 326 | 242 | 384 | 316 | 506 | 412 | 768 | 712 | 932 | 1018 | 1000 |
| 0.4 | 84 | 92 | 168 | 256 | 198 | 312 | 244 | 358 | 296 | 428 | 444 | 524 | 1004 | 634 |
| 0.6 | -- | 66 | -- | 278 | -- | 494 | -- | 658 | -- | 766 | -- | 886 | -- | 1012 |
| 0.8 | 76 | -- | 218 | -- | 268 | -- | 362 | -- | 562 | -- | 756 | -- | 796 | -- |
| Avg. | 77 | | 243 | | 320 | | 414 | | 539 | | 685 | | 913 | |

**Table 3.3. Time in seconds to achieve a specified level of probability of representing grain size fraction using temporary stabilization. Times were recorded from the cumulative probability curves of Sites 1 and 2. Each variable is depth averaged for the associated probability level.**

| h | 50% | | 75% | | 80% | | 85% | | 90% | | 95% | | 99% | |
|---|---|---|---|---|---|---|---|---|---|---|---|---|---|---|
| | Site 1 | Site 2 | Site 1 | Site 2 | Site 1 | Site 2 | Site 1 | Site 2 | Site 1 | Site 2 | Site 1 | Site 2 | Site 1 | Site 2 |
| D10 | | | | | | | | | | | | | | |
| 0.1 | 58 | 32 | 392 | 156 | 472 | 206 | 526 | 252 | 660 | 384 | 748 | 608 | 1016 | 930 |
| 0.2 | 44 | 74 | 176 | 200 | 214 | 236 | 260 | 318 | 644 | 520 | 734 | 622 | 1018 | 986 |
| 0.4 | 122 | 76 | 256 | 194 | 296 | 254 | 400 | 302 | 488 | 420 | 666 | 840 | 962 | 982 |
| 0.6 | -- | 46 | -- | 158 | -- | 212 | -- | 308 | -- | 544 | -- | 772 | -- | 998 |
| 0.8 | 90 | -- | 252 | -- | 310 | -- | 458 | -- | 818 | -- | 912 | -- | 1002 | -- |
| Avg. | 67.75 | | 223 | | 275 | | 353 | | 559.75 | | 737.75 | | 986.75 | |
| D16 | | | | | | | | | | | | | | |
| 0.1 | 60 | 28 | 410 | 148 | 482 | 206 | 554 | 258 | 662 | 440 | 792 | 624 | 984 | 928 |
| 0.2 | 52 | 70 | 180 | 196 | 212 | 222 | 298 | 298 | 498 | 500 | 704 | 606 | 1018 | 962 |
| 0.4 | 110 | 88 | 242 | 206 | 282 | 256 | 376 | 312 | 466 | 426 | 712 | 526 | 964 | 900 |
| 0.6 | -- | 56 | -- | 292 | -- | 414 | -- | 542 | -- | 676 | -- | 794 | -- | 998 |
| 0.8 | 80 | -- | 212 | -- | 264 | -- | 386 | -- | 680 | -- | 762 | -- | 1004 | -- |
| Avg. | 68 | | 235.75 | | 292.25 | | 378 | | 543.5 | | 690 | | 969.75 | |
| D50 | | | | | | | | | | | | | | |
| 0.1 | 44 | 26 | 376 | 106 | 482 | 170 | 600 | 242 | 738 | 332 | 824 | 544 | 1002 | 774 |
| 0.2 | 54 | 66 | 198 | 180 | 266 | 212 | 330 | 288 | 460 | 432 | 562 | 558 | 1012 | 620 |
| 0.4 | 78 | 136 | 170 | 390 | 204 | 476 | 286 | 544 | 358 | 636 | 548 | 870 | 932 | 952 |
| 0.6 | -- | 72 | -- | 432 | -- | 534 | -- | 660 | -- | 758 | -- | 870 | -- | 1006 |
| 0.8 | 90 | -- | 244 | -- | 328 | -- | 434 | -- | 754 | -- | 910 | -- | 994 | -- |
| Avg. | 70.75 | | 262 | | 334 | | 423 | | 558.5 | | 710.75 | | 911.5 | |
| D84 | | | | | | | | | | | | | | |
| 0.1 | 42 | 32 | 256 | 126 | 350 | 160 | 466 | 224 | 682 | 304 | 786 | 392 | 854 | 492 |
| 0.2 | 54 | 78 | 174 | 188 | 242 | 216 | 296 | 298 | 370 | 450 | 674 | 564 | 1014 | 606 |
| 0.4 | 78 | 84 | 166 | 234 | 198 | 288 | 246 | 346 | 298 | 408 | 502 | 518 | 1004 | 980 |
| 0.6 | -- | 68 | -- | 344 | -- | 542 | -- | 674 | -- | 780 | -- | 902 | -- | 1002 |
| 0.8 | 76 | -- | 234 | -- | 308 | -- | 380 | -- | 542 | -- | 762 | -- | 802 | -- |
| Avg. | 64 | | 215.25 | | 288 | | 366.25 | | 479.25 | | 637.5 | | 844.25 | |

| h | 50% | | 75% | | 80% | | 85% | | 90% | | 95% | | 99% | |
|---|---|---|---|---|---|---|---|---|---|---|---|---|---|---|
| | Site 1 | Site 2 | Site 1 | Site 2 | Site 1 | Site 2 | Site 1 | Site 2 | Site 1 | Site 2 | Site 1 | Site 2 | Site 1 | Site 2 |
| D90 | | | | | | | | | | | | | | |
| 0.1 | 44 | 54 | 202 | 210 | 248 | 262 | 336 | 310 | 596 | 444 | 682 | 688 | 964 | 856 |
| 0.2 | 54 | 106 | 142 | 304 | 200 | 342 | 272 | 452 | 336 | 676 | 494 | 902 | 740 | 1000 |
| 0.4 | 70 | 74 | 164 | 216 | 192 | 260 | 238 | 322 | 296 | 378 | 464 | 472 | 1002 | 984 |
| 0.6 | -- | 66 | -- | 308 | -- | 556 | -- | 682 | -- | 806 | -- | 914 | -- | 986 |
| 0.8 | 78 | -- | 266 | -- | 340 | -- | 420 | -- | 520 | -- | 786 | -- | 840 | -- |
| Avg. | 68.25 | | 226.5 | | 300 | | 379 | | 506.5 | | 675.25 | | 921.5 | |

# 4.0. Discussion

**Do current point-sample measurement techniques adequately capture a representative value of suspended sediment?**

According to the Water Survey of Canada Field Guide, the time required to fill a quart-sized bottle with a USGS standard P-63 at flows averaging 1.0 – 1.8 m $s^{-1}$ as observed during our data collection, is 20 – 41 seconds [Tassone and Lapointe, 1999]. According to our findings a measurement in this time period presents on average 35 – 45% probability of accurately reflecting the long-term mean concentration or grain size fraction. Times presented in Tables 3.2 and 3.3 for each variable are depth averaged to obtain a single estimate of sample duration for a given level of probability. Collection of the volumetric concentration with 90% confidence of accurately representing the mean value requires 570 seconds (9.5 minutes) of sampling. Alternatively stated, if one were to collect ten 9.5 minutes samples, one of those samples is likely to be unrepresentative. If two bottle samples of volumetric concentration were collected to represent the mean concentration, each 40 seconds in length, statistically, only one of the bottles would accurately represent the mean concentration. Clearly, the time averaging performed during the collection of a standard bottle sample is insufficient to accurately reflect the long-term mean value. Inadequate time averaging as a source of error in depth-integrated bottle sampling identified in Topping et al. [2011] also influences point-sample measurements. Typical short-duration bottle samples capture some of the variability of the long-term average but do not guarantee a representative sample. Topping et al. [2011] recommended adding a second transit, which by sampling the same location twice improves time averaging at every point in the flow. In point sample measurements, time averaging at a single point is considerably greater than in depth-integration but it is clear that the time averaging performed during a single sample is not long enough. Therefore, the results suggest that current bottle sampling practices are insufficient to capture the true mean concentration or grain size fraction in suspension. The probability of a single bottle sample accurately reflecting the mean concentration or grain size

fraction is too low to consider that the current methods are a reasonable sampling approach and is one of the reasons for the customary large scatter in suspended sediment rating curves. Increasing the time period over which suspended sediment is measured therefore seems to be the most appropriate way to improve the probability of representing the long-term mean concentration or grain size fraction.

**What sample duration is required to obtain an accurate mean concentration? Does the time required to obtain a representative mean concentration vary for different components of the suspended sediment load?**

Guaranteeing certainty in a measurement accurately reflecting the long-term value is difficult. Long-duration measurements are equal to the measurement period and are the best approach to accurately representing the long-term value but due to exceedingly long measurement times this is impractical. Assuming a lower probability still requires exceptionally long sample durations; a total of nineteen bottle samples, each collecting 30 seconds of water-sediment mixture would be required to provide a 90% probability of accurately representing the mean concentration of volumetric concentration. Currently a single bottle sample is used for each point in the water column to provide the mean concentration. Results from these structured observations indicate this approach may be accurate in <50% of samples. The results also indicate that the probability of obtaining a representative mean concentration or grain size moment is approximately the same for all variables meaning the same measurement period may be appropriate for all components of the suspended sediment load and all grain size fractions. Improving the probability of representing the long-term value in the shortest period of time would bridge the gap between short duration, moderately probable estimates of the long-term value and prohibitively long, but certain measurements.

By locating the point of diminishing returns on the cumulative probability curves we are able to determine a sampling time adequate to maximize sampling efficiency while minimizing sampling time. Finding this point of diminishing returns in sampling time is accomplished by identifying the break in slope along each line of cumulative probability. In all plots there is an immediate increase in probability for the first 2 minutes and a lower rate of increase beyond the 8-minute mark. The point of diminishing returns

occurs between these two periods. Measuring the slope of each of these segments and identifying the point at which they intersect identifies the point of diminishing returns. This point indicates the most efficient duration over which to sample and the probability associated with the measurement time is obtained from the cumulative probability curve.

Using the point of diminishing returns a depth-averaged value of the most efficient sampling time can be reached. The most efficient sample of volumetric concentration will be collected by 264 seconds with 73% probability of accurately representing the mean. For $D_{50}$ a sample must be 240 seconds long to achieve 75% probability. Summary of all other variables can be found in Appendix D. The method involving the point of diminishing returns does not indicate how long a sample should be collected for but rather indicates the shortest sample duration likely to ensure the greatest probability of accurately reflecting the mean concentration of grain size fraction of interest.

The length of sample required to accurately represent the mean concentration of a suspended sediment load or a particular grain size fraction depends on the level of probability desired. Since individual bottle samples bear a low probability of representing the mean value, requiring multiple bottles totalling between 9 and 12 minutes of sample duration to accurately reflect the mean, it becomes evident that bottle sampling may not be the most efficient method of sampling suspended sediment. This research indicates that longer duration sampling through alternative means may prove more effective while being less time consuming and resource demanding than traditional bottle sampling. Collection of continuous suspended sediment data has been successfully documented using acoustic monitoring [Attard et al., 2014]. Pressure-difference techniques [Gray and Landers, 2014] may also provide continuous data. Laser-diffraction, used in this research, also provides continuous concentration data.

# 5.0. Conclusion

Long duration measurements of suspended sediment concentration were examined from the Fraser River, British Columbia, Canada. Continuous hour-long time series data of suspended sediment concentration and grain size distribution were collected along two sampling profiles based on a standard sampling profile. Average discharge was 8265 $m^3$ $s^{-1}$ during the measurement period May 30 – June 2, 2013. A probability-based approach determined the likelihood of a sample of suspended sediment accurately reflecting the long-term value of mean concentration or grain size fraction. Results indicate that typical bottle samples of <60 seconds in duration bear a low to moderate probability of accurately representing the long-term value. Improving the probability to 90 % of accurately reflecting the mean concentration of volumetric concentration requires 9.5 minutes of sampling duration. All components of the suspended load and grain size fractions bear approximately the same likelihood of representing the long-term value for any given time period. The results indicate that current bottle sampling measurement techniques inadequately time-average over the variability in suspended sediment concentration and do no reliably provide a representative mean concentration.

# References


Adrian, R. J., and Marusic, I. (2012). Coherent structures in flow over hydraulic engineering surfaces. Journal of Hydraulic Research, 50:5, 451–464.

Adrian, R. J. (2013). Structure of Turbulent Boundary Layers. In Coherent Flow Structures at Earth's Surface (pp. 17–24).

Attard, M. E. (2012). Evaluation of ADCPs for suspended sediment transport monitoring, Fraser River, British Columbia. MSc thesis, Simon Fraser University.

Attard, M. E., Venditti, J. G., and Church, M. (2014). Suspended sediment transport in Fraser River at Mission, British Columbia: New observations and comparison to historical records. Canadian Water Resources Journal / Revue Canadienne Des Ressources Hydriques, 39(3), 356–371. doi:10.1080/07011784.2014.942105

Bendat, J. S., and Piersol, A. G. (1966). Measurement and analysis of random data. USA: John Wiley and Sons. (pp. 337 – 344)

Bradley, R. W., Venditti, J. G., Kostaschuk, R. A., Hendershot, M., Church, M., and Columbia, B. (2013). Flow and sediment suspension events over low-angle dunes : Fraser Estuary, Canada. Journal of Geophysical Research. 118, 1693-1709, doi:10.1002/jgrf.20118

Bridge, J. S. (2003). Rivers and floodplains: forms, processes, and sedimentary record. USA: Blackwell Science Ltd. (pp. 55 – 56)

Church, M. (2006). Bed Material Transport and the Morphology of Alluvial River Channels. Annual Review of Earth and Planetary Sciences, 34(1), 325–354. doi:10.1146/annurev.earth.33.092203.122721

Dashtgard, S. E., Venditti, J. G., Hill, P. R., Sisulak, C. F., Johnson, S. M., and La Croix, A. D. (2012). Sedimentation across the tidal-fluvial transition in the lower Fraser River, Canada. The Sedimentary Record, 4–9. doi: 10.2110/sedred.2012.4

Domarad, N. (2011). Flow and suspended sediment transport through the gravel-sand transition in the Fraser River, British Columbia. M.Sc. thesis, Simon Fraser University.

Hutchins, N., and Marusic, I. (2007). Evidence of very long meandering features in the logarithmic region of turbulent boundary layers. Journal of Fluid Mechanics, 579, 1. doi:10.1017/S0022112006003946

Gray, T. E., Alexander, J., & Leeder, M. R. (2005). Quantifying velocity and turbulence structure in depositing sustained turbidity currents across breaks in slope. Sedimentology, 52(3), 467–488. doi:10.1111/j.1365-3091.2005.00705.x

Gray, J. R. and Landers, M. N. (2014). Measuring suspended sediment. In Ahuja, S., editor, Comprehensive Water Quality and Purification. Amsterdam, Elsevier, vol. 1, 157-204.

Kline, S. J., Reynolds, W. C., Schraub, F. A., and Rundstadler, P. W. (1967). The structure of turbulent boundary layers. Journal of Fluid Mechanics, 30, 741–773.

Kostaschuk, R. a., and Church, M. a. (1993). Macroturbulence generated by dunes: Fraser River, Canada. Sedimentary Geology, 85, 25–37. doi:10.1016/0037-0738(93)90073-E

Kostaschuk, R., and Best, J. (2005). Response of sand dunes to variations in tidal flow: Fraser Estuary, Canada. Journal of Geophysical Research, 110. doi:10.1029/2004JF000176

Kwoll, E., Becker, M., and Winter, C. (2014). With or against the tide: The influence of bed form asymmetry on the formation of Macroturbulence and suspended sediment patterns. Water Resources Research, 2108–2123. doi:10.1002/2012WR013085.

Lapointe, M. (1992). Burst-like sediment suspension events in a sand bed river. Earth Surface Processes and Landforms, 17(3), 253–270. doi:10.1002/esp.3290170305

Lapointe, M. (1993). Monitoring alluvial sand suspension by eddy correlation. Earth Surface Processes and Landforms, 18, 157–175. doi: 10.1002/esp.3290180207

Lapointe, M. F. (1996). Frequency spectra and intermittency of the turbulent suspension process in a sand-bed river. Sedimentary Geology, 43, 439–449. doi:10.1046/j.1365-3091.1996.d01-18.x

Marquis, G. A., & Roy, A. G. (2013). From macroturbulent flow structures to large- scale flow pulsations in gravel- bed rivers. Coherent Flow Structures at Earth's Surface, (pp. 261-274).

McLean, D. G., Church, M., and Tassone, B. (1999). Sediment transport along lower Fraser River: 1. Measurements and hydraulic computations. Water Resources Research, 35(8), 2533. doi:10.1029/1999WR900101

Menke, W., and Menke, J. (2012). Environmental data analysis with MATLAB. USA: Elsevier. (pp. 229 – 234).

Milliman, J. D., and Meade, R. H. (1983). World-wide delivery of river sediment to the oceans. The Journal of Geology. doi:10.1086/628741

Milliman, J. D., and Syvitski, J. P. M. (1992). Geomorphic/tectonic control of sediment discharge to the ocean: the importance of small mountainous rivers. Journal of Geology, 100, 325–344.

Schmid, H. (2012). How to use the FFT and Matlab's pwelch function for signal and noise simulations and measurements. [Report]. Retrieved from http://www.fhnw.ch/technik/ime/publikationen/2012/how-to-use-the-fft-and-matlab2019s-pwelch-function-for-signal-and-noise-simulations-and-measurements (accessed on 10 July, 2014).

Sequoia Scientific Inc. (2013). LISST-SL V2.1 Operating manual. Retrieved from http://www.sequoiasci.com/wp-content/uploads/2013/07/LISST-SLUsersManual_v2.1.pdf (accessed on 5 May, 2013).

Shugar, D. H., Kostaschuk, R., Best, J. L., Parsons, D. R., Lane, S. N., Orfeo, O., and Hardy, R. J. (2010). On the relationship between flow and suspended sediment transport over the crest of a sand dune, Río Paraná, Argentina. Sedimentology, 57(1), 252–272. doi:10.1111/j.1365-3091.2009.01110.x

Soulsby, R. (1980). Selecting record length and digitization rate for near-bed turbulence measurements. Journal of Physical Oceanography, 10, 208–219.

Syvitski, J. P., Vörösmarty, C. J., Kettner, A. J., & Green, P. (2005). Impact of humans on the flux of terrestrial sediment to the global coastal ocean. Science, 308(5720), 376-380.

Tassone, B., and Lapointe, F. (1999). Suspended-sediment sampling. Hydrometric technician career development program. The Water Survey of Canada. Retrieved from http://publications.gc.ca/collections/collection_2014/ec/En56-247-1999-eng.pdf (accessed 17 February, 2015).

Topping, D. J., Rubin, D.M., Wright, S.A., Melis, T. S. (2011). Field Evaluation of the Error Arising from Inadequate Time Averaging in the Standard Use of Depth-Integrating Suspended-Sediment Samplers. (No. 1774, pp.i-95). US Geological Survey.

Venditti, J. G., and Church, M. (2014). Morphology and controls on the position of a gravel-sand transition: Fraser River, British Columbia. Journal of Geophysical Research, 1959–1976. doi:10.1002/2014JF003147.

Venditti, J. G., Domarad, N., Church, M., & Rennie, C. D. (2015). The Gravel- sand transition: Sediment dynamics in a diffuse extension. Journal of Geophysical Research: Earth Surface. doi: 10.1002/2014JF003328.

# Appendix A.

# Power spectral estimates of suspended sediment load

### Volumetric Concentration

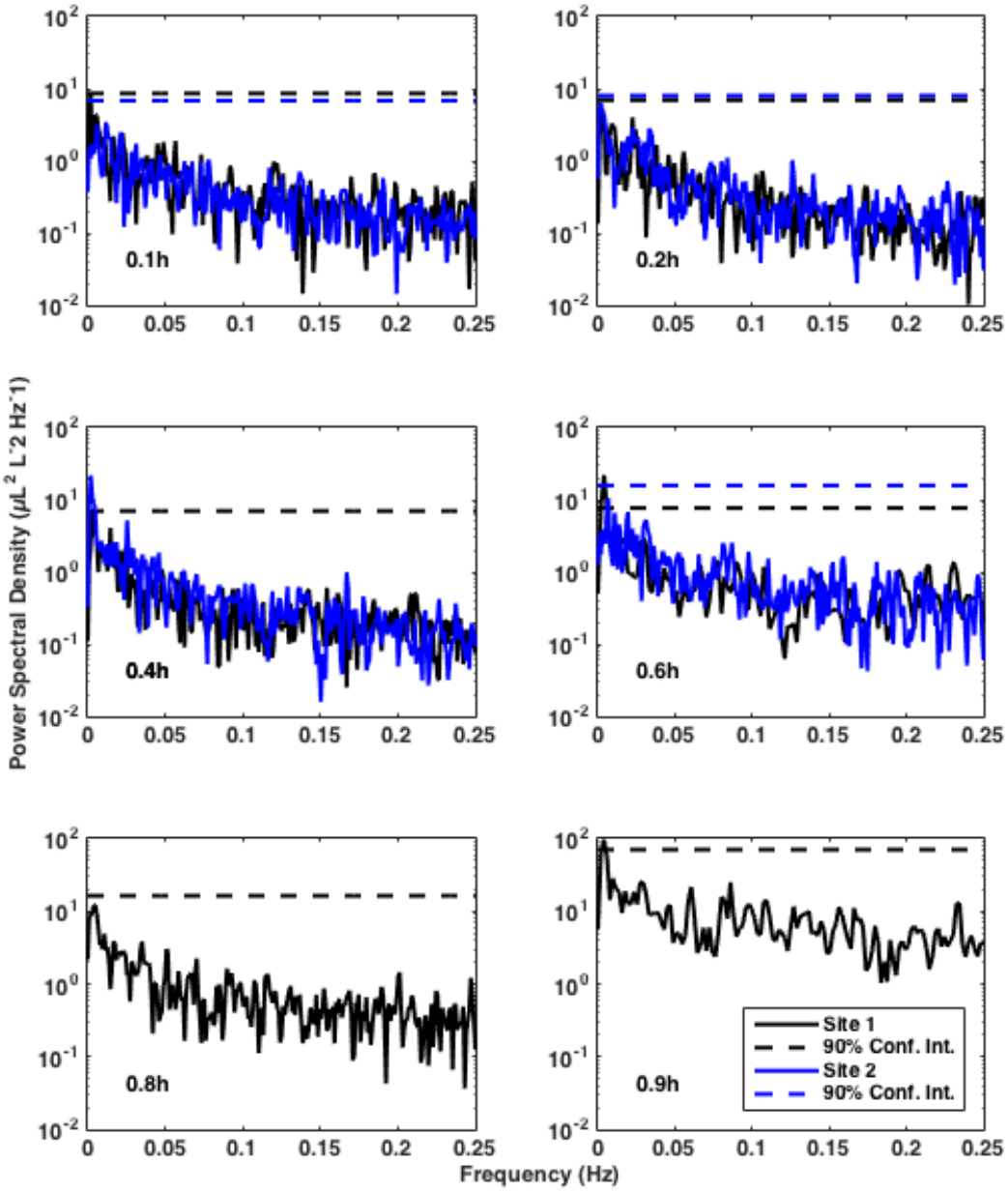


**Figure A.1.** **Power spectral density estimates for the volumetric concentration signal. Low frequency spectral peaks are rare.**

**Silt load**

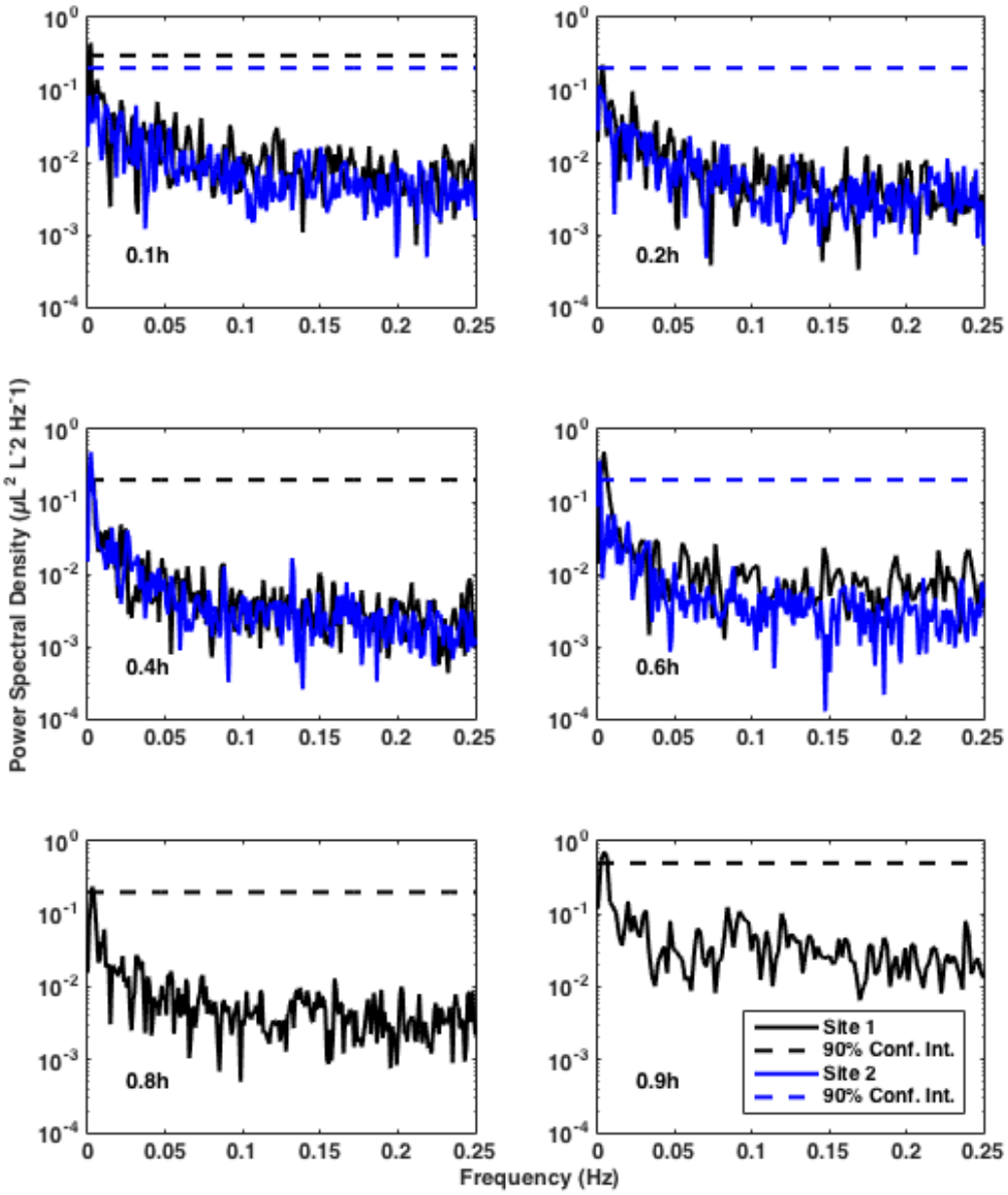


**Figure A.2. Power spectral density estimates for the silt load concentration signal. Low frequency spectral peaks are rare.**

**Sand load**

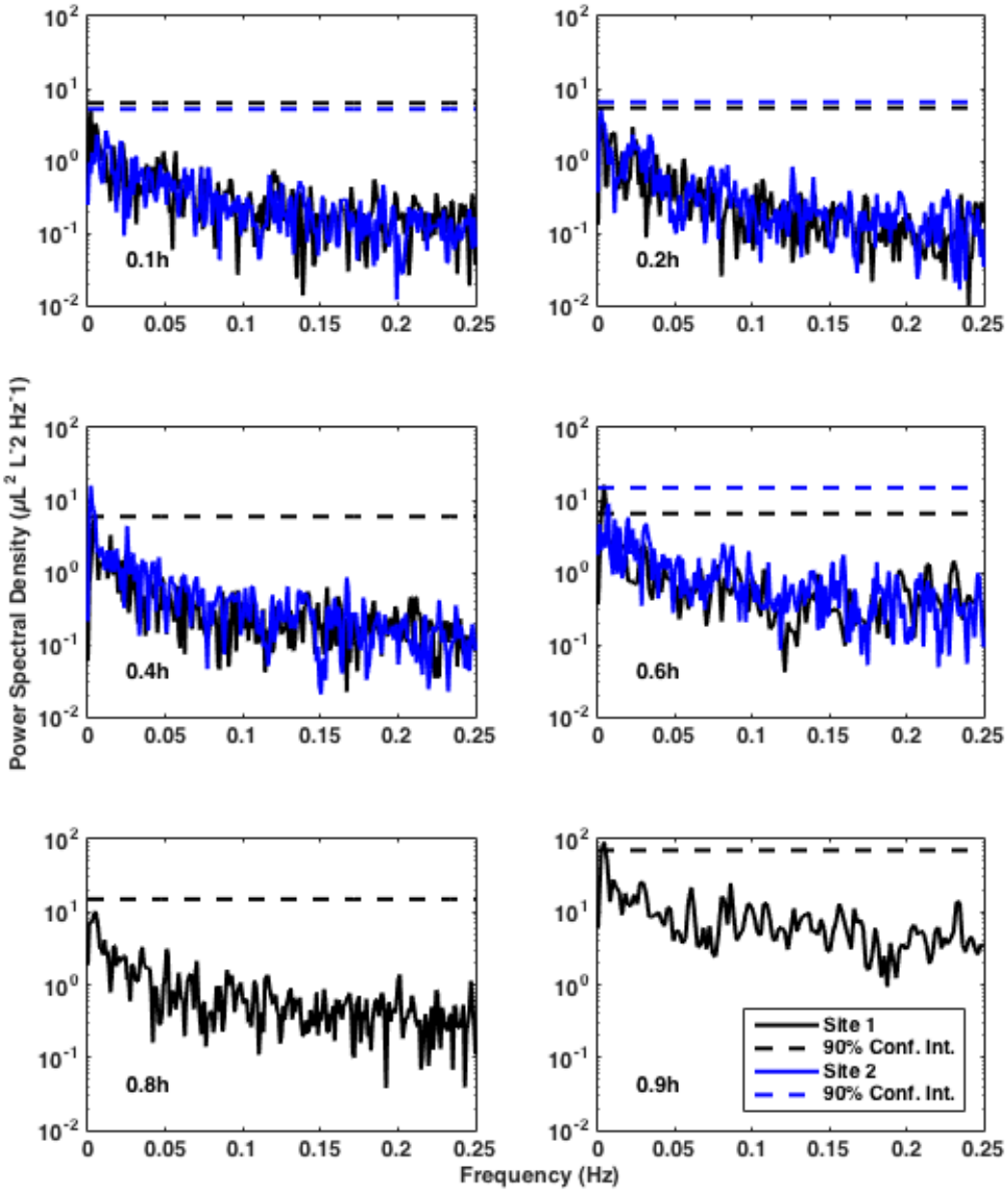


**Figure A.3. Power spectral density estimates for the sand load concentration signal. Low frequency spectral peaks are rare.**

## Washload

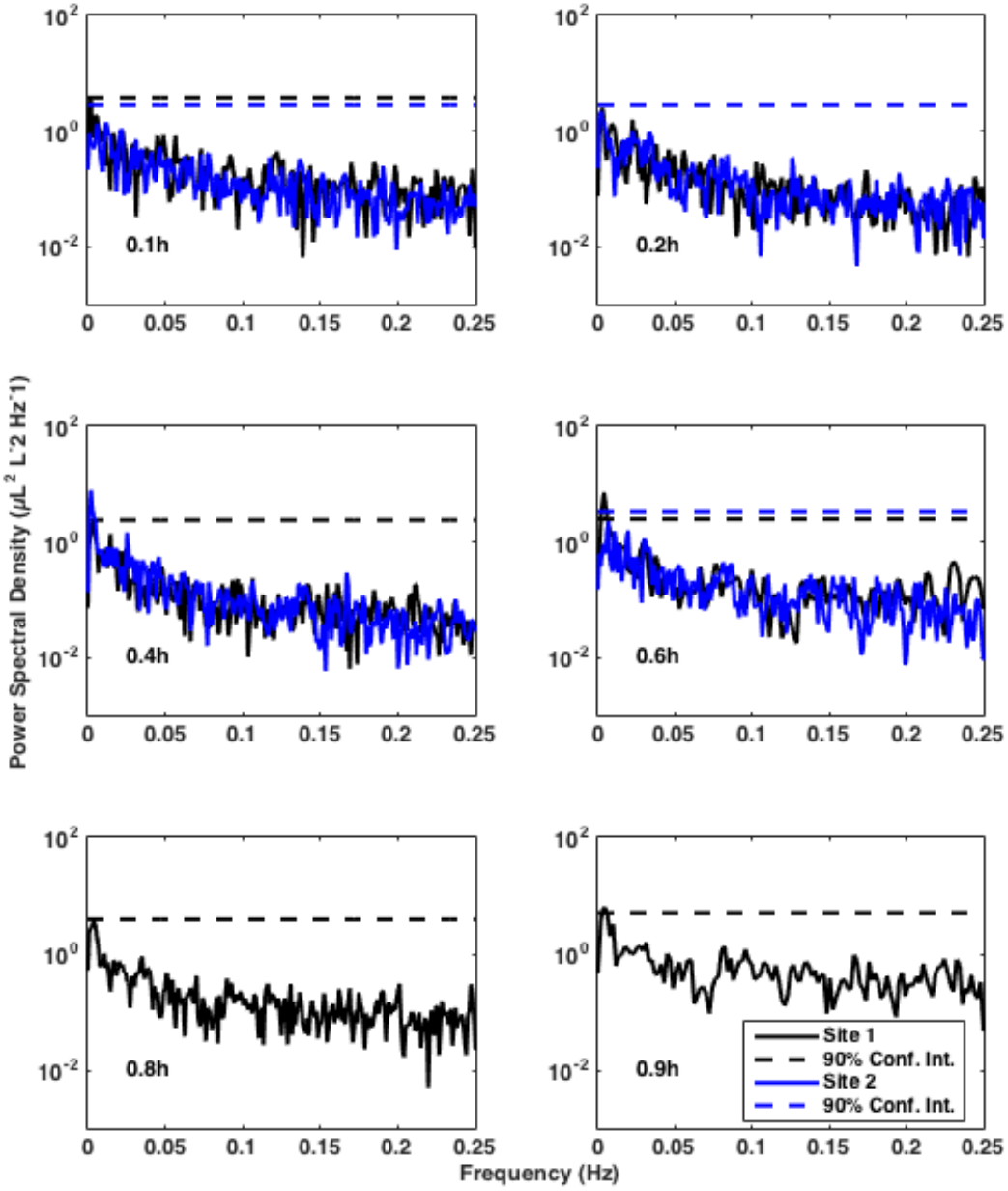


**Figure A.4. Power spectral density estimates for the washload concentration signal. Low frequency spectral peaks are rare.**

## Suspended bed material

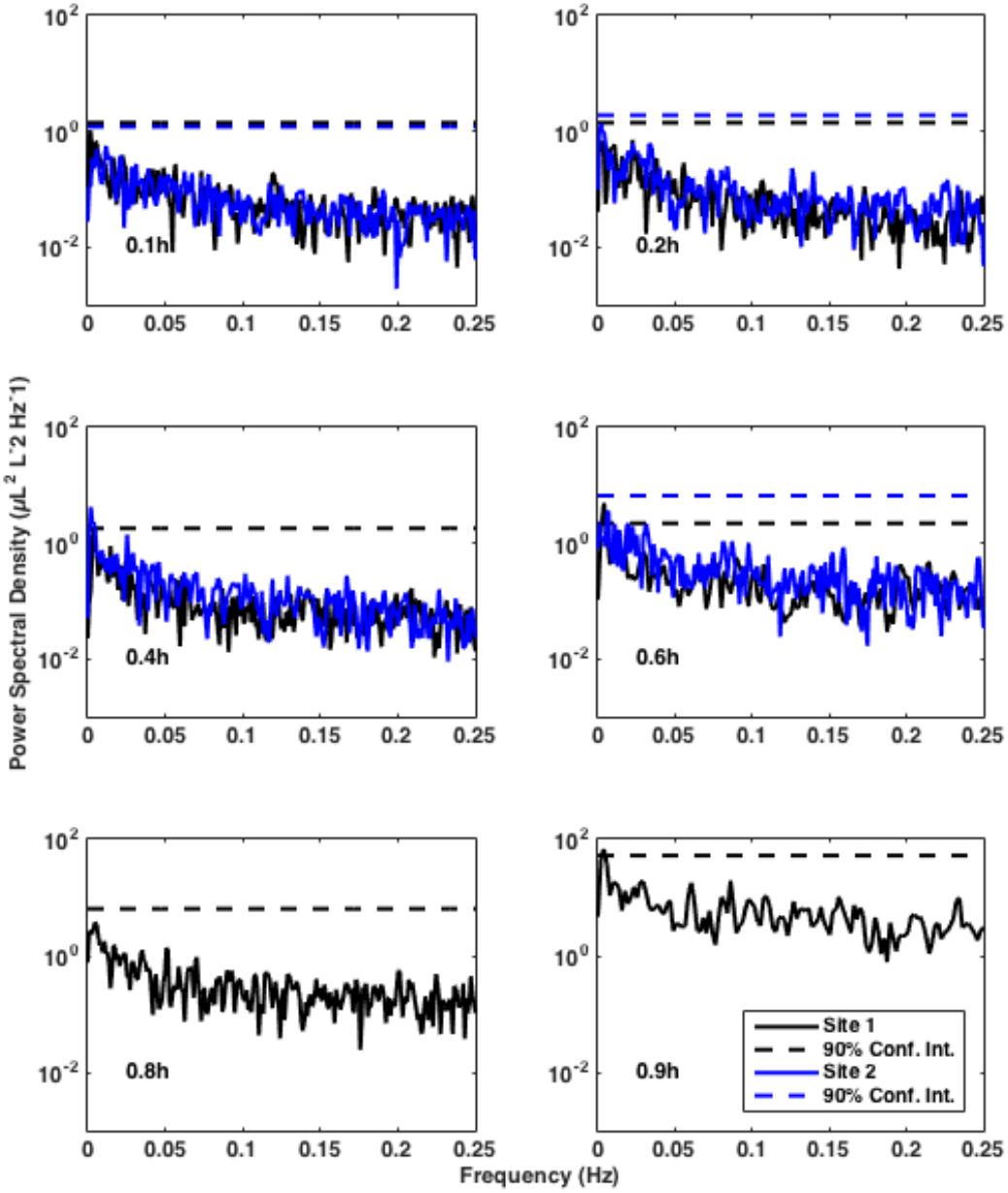


**Figure A.5.** **Power spectral density estimates for the suspended bed material concentration signal. Low frequency spectral peaks are rare.**

***D*50**

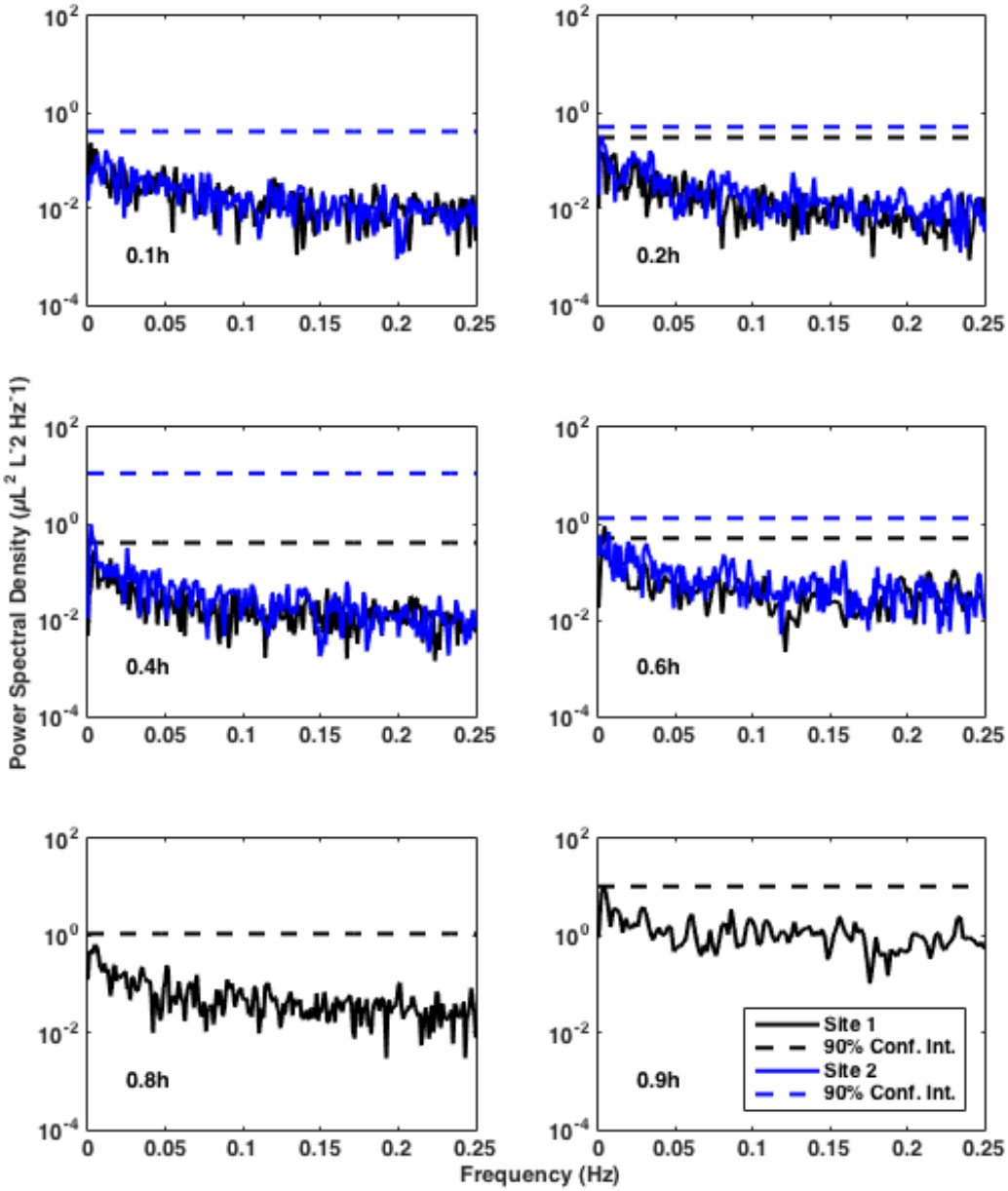


**Figure A.6. Power spectral density estimates for the *D*50 signal. Low frequency spectral peaks are rare.**

# Appendix B.

# Persistent stabilization of β

## Suspended sediment loads

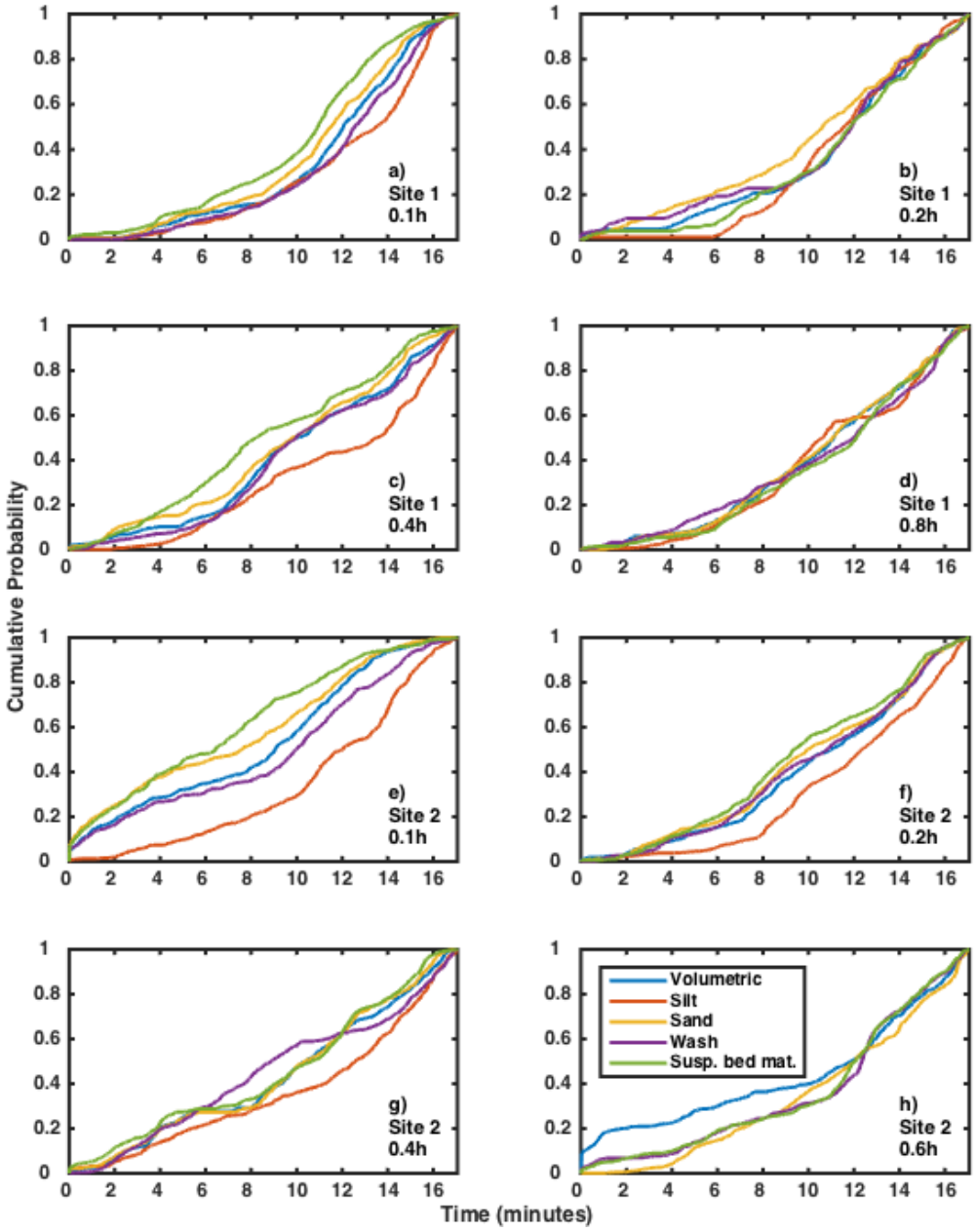


**Figure B.1.** **Cumulative probability plots of suspended sediment loads with the condition of persistent stabilization of the β signal. Measurements from Site 1 at a) 0.1*h*, b) 0.2*h*, c) 0.4*h*, d) 0.8*h*, and Site 2 at e) 0.1*h*, f) 0.2*h*, g) 0.4*h*, and h) 0.6*h*, show the cumulative probability of obtaining a sample with a representative mean value when measuring for a given period of time. These results require persistent stabilization of the mean value on the long-term mean value.**

## Grain size fractions

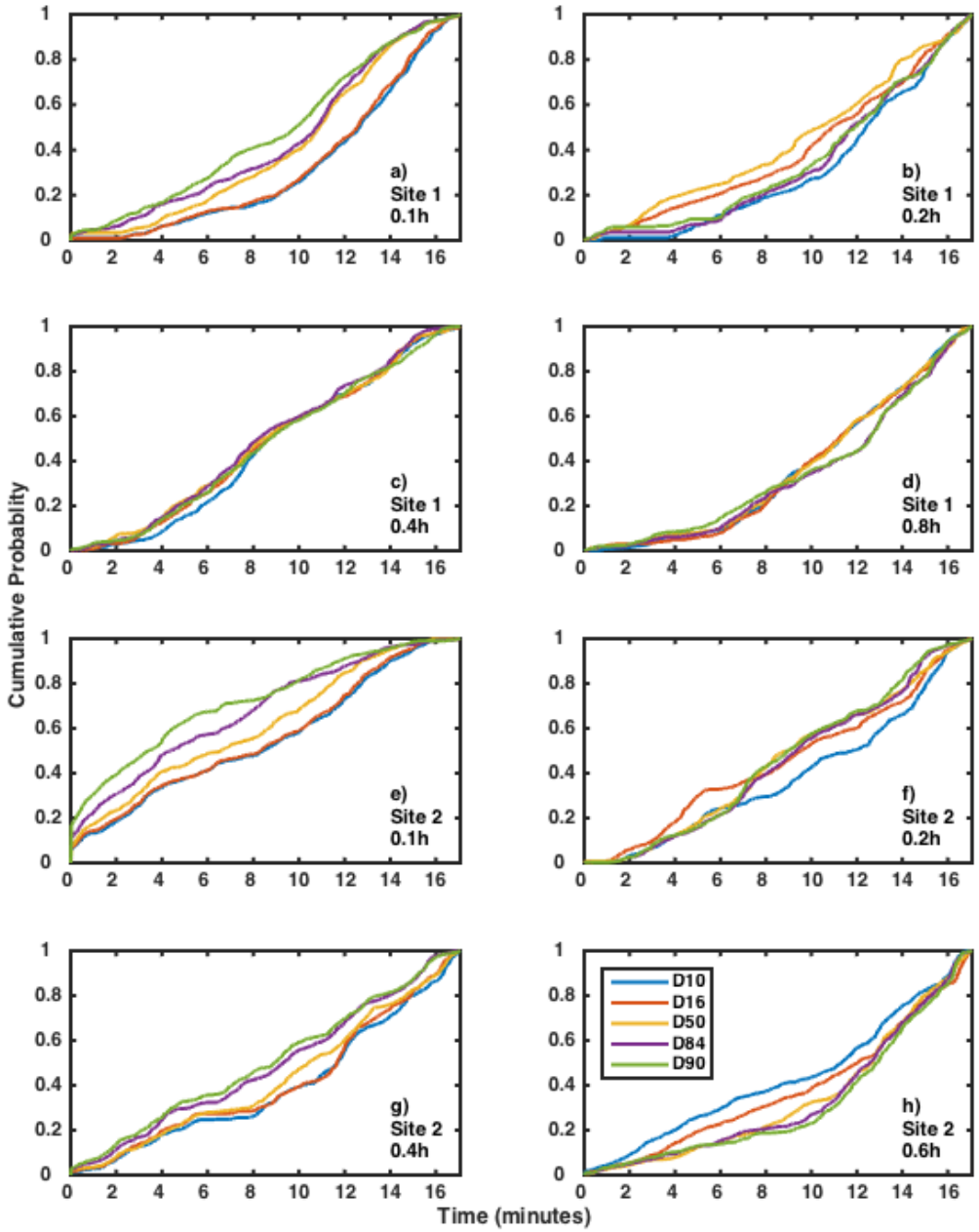


**Figure B.2.** **Cumulative probability plots of grain size fractions from Site 1 with the condition of persistent stabilization of the β signal. Measurements from Site 1 at a) 0.1*h*, b) 0.2*h*, c) 0.4*h*, d) 0.8*h*, and Site 2 at e) 0.1*h*, f) 0.2*h*, g) 0.4*h*, and h) 0.6*h*, show the cumulative probability of obtaining a sample with a representative mean value when measuring for a given period of time. These results require persistent stabilization of the mean value on the long-term mean value.**

# Appendix C.

# Sampling time for a specified level of probability

### Suspended sediment loads

| h | 50% | | 75% | | 80% | | 85% | | 90% | | 95% | | 99% | |
|---|---|---|---|---|---|---|---|---|---|---|---|---|---|---|
| | Site 1 | Site 2 | Site 1 | Site 2 | Site 1 | Site 2 | Site 1 | Site 2 | Site 1 | Site 2 | Site 1 | Site 2 | Site 1 | Site 2 |
| VOLUMETRIC CONCENTRATION | | | | | | | | | | | | | | |
| 0.1 | 724 | 506 | 852 | 738 | 874 | 764 | 890 | 804 | 914 | 838 | 950 | 900 | 1020 | 956 |
| 0.2 | 712 | 706 | 852 | 884 | 864 | 904 | 902 | 926 | 946 | 948 | 1002 | 968 | 1016 | 1008 |
| 0.4 | 602 | 702 | 860 | 870 | 880 | 898 | 900 | 944 | 946 | 980 | 986 | 998 | 1010 | 1016 |
| 0.6 | | 680 | | 838 | | 878 | | 934 | | 968 | | 980 | | 1000 |
| 0.8 | 668 | | 858 | | 892 | | 916 | | 946 | | 972 | | 1010 | |
| Avg. | 662.5 | | 844 | | 869.25 | | 902 | | 935.75 | | 969.5 | | 1004.5 | |
| SILT LOAD | | | | | | | | | | | | | | |
| 0.1 | 810 | 502 | 910 | 720 | 928 | 754 | 942 | 786 | 952 | 830 | 972 | 888 | 1004 | 944 |
| 0.2 | 694 | 574 | 832 | 864 | 892 | 884 | 916 | 902 | 944 | 932 | 968 | 962 | 1020 | 1004 |
| 0.4 | 812 | 700 | 932 | 844 | 952 | 894 | 968 | 922 | 984 | 964 | 1000 | 982 | 1018 | 1010 |
| 0.6 | | 720 | | 882 | | 914 | | 960 | | 990 | | 1002 | | 1018 |
| 0.8 | 638 | | 880 | | 904 | | 924 | | 944 | | 974 | | 1022 | |
| Avg. | 681.25 | | 858 | | 890.25 | | 915 | | 942.5 | | 968.5 | | 1005 | |
| SAND LOAD | | | | | | | | | | | | | | |
| 0.1 | 690 | 262 | 824 | 528 | 846 | 576 | 872 | 686 | 898 | 758 | 934 | 818 | 1018 | 956 |
| 0.2 | 638 | 560 | 820 | 832 | 846 | 856 | 884 | 878 | 950 | 890 | 998 | 930 | 1020 | 1008 |
| 0.4 | 590 | 558 | 820 | 764 | 848 | 838 | 882 | 886 | 902 | 918 | 952 | 940 | 1010 | 994 |
| 0.6 | | 754 | | 886 | | 918 | | 948 | | 970 | | 982 | | 1006 |
| 0.8 | 664 | | 854 | | 886 | | 912 | | 948 | | 976 | | 1012 | |
| Avg. | 589.5 | | 791 | | 826.75 | | 868.5 | | 904.25 | | 941.25 | | 1003 | |
| WASHLOAD | | | | | | | | | | | | | | |
| 0.1 | 754 | 396 | 878 | 654 | 900 | 690 | 914 | 728 | 934 | 766 | 966 | 838 | 1016 | 930 |
| 0.2 | 714 | 538 | 834 | 820 | 868 | 862 | 894 | 892 | 952 | 922 | 1002 | 968 | 1014 | 1012 |
| 0.4 | 600 | 626 | 872 | 818 | 894 | 882 | 928 | 924 | 964 | 968 | 990 | 988 | 1014 | 1014 |
| 0.6 | | 760 | | 872 | | 898 | | 938 | | 974 | | 990 | | 1012 |
| 0.8 | 722 | | 898 | | 926 | | 938 | | 952 | | 976 | | 1016 | |
| Avg. | 638.75 | | 830.75 | | 865 | | 894.5 | | 929 | | 964.75 | | 1003.5 | |

| h | 50% | | 75% | | 80% | | 85% | | 90% | | 95% | | 99% | |
|---|---|---|---|---|---|---|---|---|---|---|---|---|---|---|
| | Site 1 | Site 2 | Site 1 | Site 2 | Site 1 | Site 2 | Site 1 | Site 2 | Site 1 | Site 2 | Site 1 | Site 2 | Site 1 | Site 2 |
| SUSPENDED BED MATERIAL | | | | | | | | | | | | | | |
| 0.1 | 656 | 202 | 768 | 524 | 792 | 588 | 826 | 638 | 870 | 706 | 926 | 820 | 1018 | 982 |
| 0.2 | 712 | 538 | 870 | 800 | 892 | 830 | 922 | 852 | 964 | 888 | 996 | 916 | 1018 | 1006 |
| 0.4 | 494 | 536 | 784 | 768 | 830 | 808 | 856 | 884 | 886 | 916 | 918 | 946 | 1012 | 1002 |
| 0.6 | | 772 | | 900 | | 932 | | 960 | | 976 | | 984 | | 1000 |
| 0.8 | 728 | | 860 | | 898 | | 926 | | 958 | | 988 | | 1010 | |
| Avg. | 579.75 | | 784.25 | | 821.25 | | 858 | | 895.5 | | 936.75 | | 1006 | |

**Table C.1. Time in seconds to achieve a specified level of probability of representing mean suspended sediment load concentration using persistent stabilization. Times were recorded from the cumulative probability curves of Sites 1 and 2. Each variable is depth averaged for the associated probability level**

## Grain size fractions

| *h* | 50% | | 75% | | 80% | | 85% | | 90% | | 95% | | 99% | |
|---|---|---|---|---|---|---|---|---|---|---|---|---|---|---|
| | Site 1 | Site 2 | Site 1 | Site 2 | Site 1 | Site 2 | Site 1 | Site 2 | Site 1 | Site 2 | Site 1 | Site 2 | Site 1 | Site 2 |
| D10 | | | | | | | | | | | | | | |
| 0.1 | 758 | 506 | 884 | 738 | 902 | 764 | 920 | 804 | 948 | 838 | 976 | 900 | 1012 | 956 |
| 0.2 | 744 | 706 | 898 | 884 | 916 | 904 | 938 | 926 | 962 | 948 | 998 | 968 | 1020 | 1008 |
| 0.4 | 522 | 702 | 788 | 870 | 816 | 898 | 854 | 944 | 886 | 980 | 926 | 998 | 1008 | 1016 |
| 0.6 | | 680 | | 838 | | 878 | | 934 | | 968 | | 980 | | 1000 |
| 0.8 | 678 | | 856 | | 886 | | 914 | | 942 | | 974 | | 1004 | |
| Avg. | 662 | | 844.5 | | 870.5 | | 904.25 | | 934 | | 965 | | 1003 | |
| D16 | | | | | | | | | | | | | | |
| 0.1 | 754 | 502 | 876 | 720 | 888 | 754 | 914 | 786 | 934 | 830 | 970 | 888 | 1012 | 944 |
| 0.2 | 652 | 574 | 870 | 574 | 888 | 574 | 920 | 574 | 952 | 574 | 990 | 574 | 1020 | 574 |
| 0.4 | 520 | 700 | 778 | 700 | 818 | 700 | 846 | 700 | 874 | 700 | 916 | 700 | 1002 | 700 |
| 0.6 | | 720 | | 720 | | 720 | | 720 | | 720 | | 720 | | 720 |
| 0.8 | 674 | | 860 | | 890 | | 926 | | 958 | | 982 | | 1008 | |
| Avg. | 637 | | 762.25 | | 779 | | 798.25 | | 817.75 | | 842.5 | | 872.5 | |
| D50 | | | | | | | | | | | | | | |
| 0.1 | 654 | 396 | 784 | 654 | 806 | 690 | 834 | 728 | 876 | 766 | 924 | 838 | 1018 | 930 |
| 0.2 | 622 | 538 | 816 | 820 | 838 | 862 | 886 | 892 | 960 | 922 | 998 | 968 | 1020 | 1012 |
| 0.4 | 508 | 626 | 784 | 818 | 830 | 882 | 856 | 924 | 876 | 968 | 906 | 988 | 1002 | 1014 |
| 0.6 | | 760 | | 872 | | 898 | | 938 | | 974 | | 990 | | 1012 |
| 0.8 | 680 | | 856 | | 888 | | 916 | | 956 | | 980 | | 1002 | |
| Avg. | 598 | | 800.5 | | 836.75 | | 871.75 | | 912.25 | | 949 | | 1001.25 | |
| D84 | | | | | | | | | | | | | | |
| 0.1 | 646 | 262 | 764 | 528 | 790 | 576 | 820 | 686 | 864 | 758 | 916 | 818 | 1004 | 956 |
| 0.2 | 706 | 560 | 884 | 832 | 914 | 856 | 938 | 878 | 964 | 890 | 992 | 930 | 1012 | 1008 |
| 0.4 | 494 | 558 | 742 | 764 | 806 | 838 | 842 | 886 | 874 | 918 | 902 | 940 | 970 | 994 |
| 0.6 | | 754 | | 886 | | 918 | | 948 | | 970 | | 982 | | 1006 |
| 0.8 | 752 | | 878 | | 918 | | 934 | | 956 | | 980 | | 1014 | |
| Avg. | 591.5 | | 784.75 | | 827 | | 866.5 | | 899.25 | | 932.5 | | 995.5 | |

| *h* | 50% | | 75% | | 80% | | 85% | | 90% | | 95% | | 99% | |
|---|---|---|---|---|---|---|---|---|---|---|---|---|---|---|
| | Site 1 | Site 2 | Site 1 | Site 2 | Site 1 | Site 2 | Site 1 | Site 2 | Site 1 | Site 2 | Site 1 | Site 2 | Site 1 | Site 2 |
| D90 | | | | | | | | | | | | | | |
| 0.1 | 592 | 202 | 744 | 524 | 782 | 588 | 816 | 638 | 868 | 706 | 928 | 820 | 1004 | 982 |
| 0.2 | 718 | 538 | 892 | 800 | 922 | 830 | 938 | 852 | 964 | 888 | 986 | 916 | 1018 | 1006 |
| 0.4 | 526 | 536 | 752 | 768 | 808 | 808 | 872 | 884 | 908 | 916 | 948 | 946 | 982 | 1002 |
| 0.6 | | 772 | | 900 | | 932 | | 960 | | 976 | | 984 | | 1000 |
| 0.8 | 756 | | 884 | | 912 | | 924 | | 946 | | 976 | | 1014 | |
| Avg. | 580 | | 783 | | 822.75 | | 860.5 | | 896.5 | | 938 | | 1001 | |

**Table C.2. Time in seconds to achieve a specified level of probability of representing grain size fractions using persistent stabilization. Times were recorded from the cumulative probability curves of Sites 1 and 2. Each variable is depth averaged for the associated probability level.**

# Appendix D.

## Point of diminishing returns

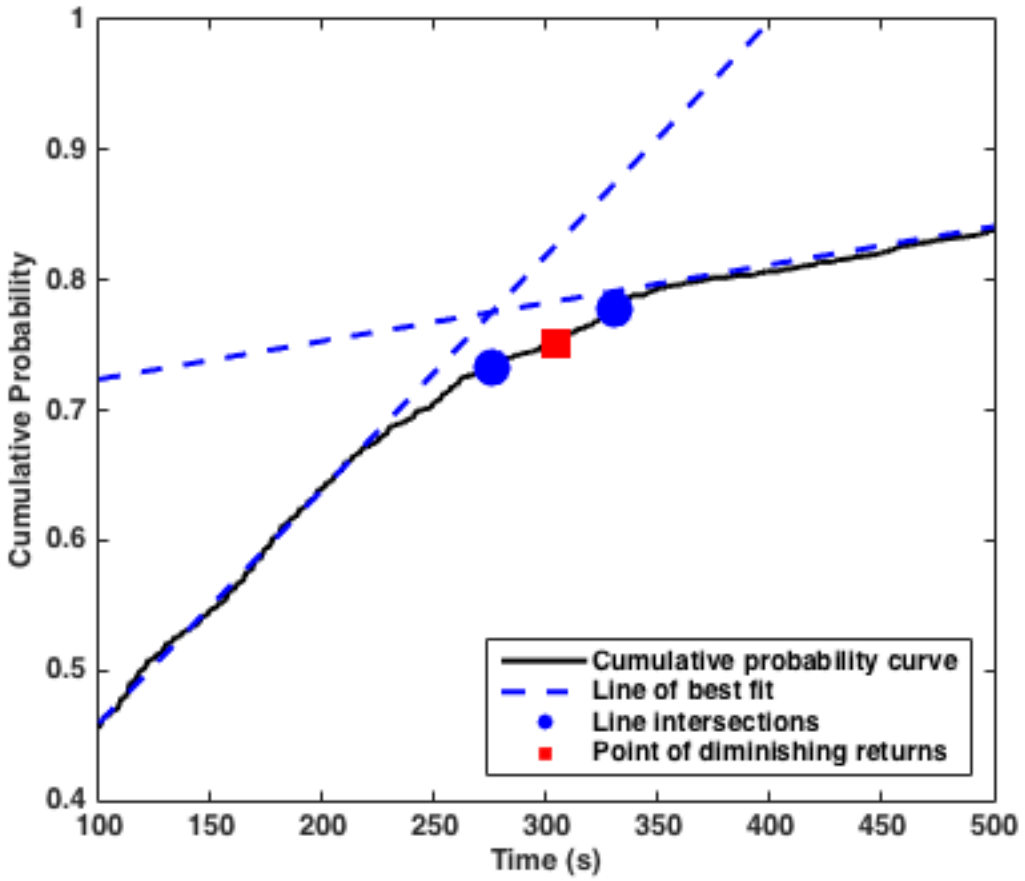


**Figure D.1.** **The point of diminishing returns is calculated by determining the line of best for the initial and terminal portions of the cumulative probability curve. Two intersections points are generated where these two lines meet; one point is directly below the intersection along the cumulative probability axis and one is directly adjacent the intersection along the time axis. The point of diminishing returns is equidistant to the line intersections.**

## Suspended sediment loads

| *h* | Volumetric | | Silt load | | Sand load | | Washload | | Suspended bed material | |
|---|---|---|---|---|---|---|---|---|---|---|
| | Time (s) | Prob. (%) | Time (s) | Prob. (%). | Time (s) | Prob. (%). | Time (s) | Prob. (%). | Time (s) | Prob. (%). |
| 0.1 | 202 | 69 | 179 | 60 | 192 | 70 | 189 | 68 | 207 | 72 |
| 0.2 | 290 | 77 | 193 | 59 | 310 | 78 | 282 | 75 | 297 | 79 |
| 0.4 | 477 | 84 | 338 | 78 | 383 | 84 | 361 | 81 | 362 | 91 |
| 0.6 | 98 | 59 | | -- | 116 | 63 | 112 | 54 | 104 | 60 |
| 0.8 | 252 | 77 | 358 | 83 | 294 | 77 | 282 | 78 | 216 | 75 |
| Avg. | 264 | 73 | 267 | 70 | 259 | 74 | 245 | 71 | 237 | 75 |

**Table D.1. Time and probability of achieving a representative sample of suspended sediment loads with respect to the point of diminishing returns.**

## Grain size fractions

| *h* | D10 | | D16 | | D50 | | D84 | | D90 | |
|---|---|---|---|---|---|---|---|---|---|---|
| | Time (s) | Prob. (%) | Time (s) | Prob. (%) | Time (s) | Prob. (%) | Time (s) | Prob. (%) | Time (s) | Prob. (%) |
| 0.1 | 227 | 74% | 169 | 70% | 162 | 72% | 239 | 79% | 202 | 74% |
| 0.2 | 189 | 76% | 231 | 80% | 274 | 83% | 289 | 83% | 258 | 77% |
| 0.4 | 353 | 86% | 382 | 87% | 373 | 83% | 380 | 91% | 362 | 92% |
| 0.6 | 182 | 78% | 152 | 65% | 114 | 58% | 106 | 58% | 98 | 57% |
| 0.8 | 242 | 74% | 166 | 70% | 278 | 78% | 270 | 78% | 268 | 75% |
| Avg. | 239 | 78% | 220 | 74% | 240 | 75% | 257 | 78% | 238 | 75% |

**Table D.2. Time and probability of achieving a representative sample of grain size fractions with respect to the point of diminishing returns.**